DeepWind Deliverable

Grant Agreement number:	**256769**
Project title:	**Future Deep Sea Wind Turbine Technologies**
Deliverable No.:	**D7.1**
Deliverable title:	**The Demonstrator-concept, design and manufacture**
Deliverable status:	**final**
Name of lead beneficiary:	**DTU**
Nature of deliverable:	**R**
Dissemination level:	**PU**
Due date from Annex 1:	**30/11/2011**
Actual submission date:	**30/5/2013, M33**

Quality check approval by: **Flemming Rasmussen** **date: 30/5-2013**

Design and Manufacture of an Offshore Concept Wind Turbine – the DeepWind Demonstrator

Troels F Pedersen, et.al.
DTU Wind Energy E-0030 May 2013

The objectives of the DeepWind project work package 7 was to design and build a demonstrator wind turbine for testing of the fundamental principles behind the wind turbine concept. The demonstrator design was achieved through two design cycles. The final design was decided to be of a configuration that is floating and is supported by a torque arm that connects the generator box to the foundation on the sea bed. The wind turbine rotor was conservatively designed as a two or three bladed Darrieus rotor rated at 1kW. The blades were designed and produced in two configurations for a 2m high and 2m diameter rotor. Three aluminium extruded blades were made in semi-circular shape and three other GRP blades were made in Troposkien shape. The 5m rotor tube was made in aluminium and was at the bottom connected to the generator box shaft with a flange. The stainless steel generator box with the 1kW generator, a mechanical drum brake and a gearing belt was mounted in a steel gimbals joint on the 5m long torque steel arm in order to allow tilt and roll movements. The torque steel arm was mounted on the steel foundation via a swivel joint to allow movements in heave. The foundation with three steel legs and concrete feet were designed to stand firmly on the seabed, but to keep the main parts above the mud. The foundation had a horizontal flange on which a steel meteorology mast was mounted. The mast had three sections, two 3m sections and a top section with fitting for a sonic anemometer. The rotor tube was mounted with a measurement system to measure movements of the rotor tube. The turbine rotor was investigated for power and loads, and a modal analysis of structural dynamics was made both theoretically and experimentally, providing evidence for a structurally safe construction.

Design and Manufacture of an Offshore Concept Wind Turbine – the DeepWind Demonstrator

DTU Vindenergi
Report 2013

Troels F Pedersen, et.al.

DTU Wind Energy E-0030

May 2013

DTU Vindenergi
Institut for Vindenergi

Authors: Troels F Pedersen, et.al., et.al.

Title: Design and Manufacture of an Offshore Concept Wind Turbine – the DeepWind Demonstrator

Institute: Wind Energy Division

Abstract (max 2000 char.):

The objectives of the DeepWind project work package 7 was to design and build a demonstrator wind turbine for testing of the fundamental principles behind the wind turbine concept. The demonstrator design was achieved through two design cycles. The final design was decided to be of a configuration that is floating and is supported by a torque arm that connects the generator box to the foundation on the sea bed. The wind turbine rotor was conservatively designed as a two or three bladed Darrieus rotor rated at 1kW. The blades were designed and produced in two configurations for a 2m high and 2m diameter rotor. Three aluminium extruded blades were made in semi-circular shape and three other GRP blades were made in Troposkien shape. The 5m rotor tube was made in aluminium and was at the bottom connected to the generator box shaft with a flange. The stainless steel generator box with the 1kW generator, a mechanical drum brake and a gearing belt was mounted in a steel gimbals joint on the 5m long torque steel arm in order to allow tilt and roll movements. The torque steel arm was mounted on the steel foundation via a swivel joint to allow movements in heave. The foundation with three steel legs and concrete feet were designed to stand firmly on the seabed, but to keep the main parts above the mud. The foundation had a horizontal flange on which a steel meteorology mast was mounted. The mast had three sections, two 3m sections and a top section with fitting for a sonic anemometer. The rotor tube was mounted with a measurement system to measure movements of the rotor tube. The turbine rotor was investigated for power and loads, and a modal analysis of structural dynamics was made both theoretically and experimentally, providing evidence for a structurally safe construction.

DTU Wind Energy E-0030

May 2013

Contract no.:

FP7 ENERGY.2010 FET

Proposal No 256769-1

Sponsorship:

EU-FP7 ENERGY.2010.10.2-1 FET

Front page:

DeepWind Demonstrator mounted for structural dynamic testing

ISBN: 978-87-92896-42-1

Pages: 74

Tables: 38

References: 13

Technical University of Denmark

DTU Wind Energy

Frederiksborgvej 399

Building 125

4000 Roskilde

trpe@dtu.dk

www.vindenergi.dtu.dk

Preface

The present summary report represents deliverable D7.1 in the DeepWind project, EU-FP7: ENERGY-2010.10.2-1 FET, Grant Agreement No 256769, project title: Future Deep Sea Wind Turbine Technologies (project website: www.deepwind.eu). The report describes design and manufacture of an offshore concept wind turbine for proof-of-concept tests. The project is financed by EU-FP7 and the work is made in a cooperation consortium between DTU, TU Delft, Aalborg University, DHI, SINTEF, Norsk Marintech, Nenuphar, Statoil, Trento University, Vestas. The design and manufacture of the demonstrator wind turbine was made as task 7.1 in work package 7, proof of principle experiments. The participants in this task were: DTU, Vestas, Aalborg University, Nenuphar, University of Trento.

The summary report represents work made by several colleagues and project partners. The following contributors should be acknowledged for splendid work:

DTU
Troels Friis Pedersen, Uwe Schmidt Paulsen, Luca Vita, Helge Aagard Madsen, Per Hørlyck Nielsen, Knud Kragh, Karen Enevoldsen, Steen Arne Sørensen, Michael Rasmussen, Rene Kjærsgaard, Claus B M Pedersen, Kasper Clemmensen

Trento University
Lorenzo Battisti, Luca Zanne, Alessandra Brighenti

Vestas
Jacob Wedell-Heinen, Victor Lim, Jiann Yi Ho, Isaac Lee

Aalborg University
Ewen Ritchie, Monika Leban Krisztina

Delft University
Gerard J. W. van Bussel
Giuseppe Tescione

DHI
Stefan Carstensen

Marintek
Petter Andreas Berthelsen

Nenuphar
Charles Smadja

Risø Campus, April 2013
Troels Friis Pedersen

Content

Abstract

The objectives of the DeepWind project work package 7 was to design and build a demonstrator wind turbine for testing of the fundamental principles behind the wind turbine concept. The demonstrator design was achieved through two design cycles. The final design was decided to be of a configuration that is floating and is supported by a torque arm that connects the generator box to the foundation on the sea bed. The wind turbine rotor was conservatively designed as a two or three bladed Darrieus rotor rated at 1kW. The blades were designed and produced in two configurations for a 2m high and 2m diameter rotor. Three aluminium extruded blades were made in semi-circular shape and three other GRP blades were made in Troposkien shape. The 5m rotor tube was made in aluminium and was at the bottom connected to the generator box shaft with a flange. The stainless steel generator box with the 1kW generator, a mechanical drum brake and a gearing belt was mounted in a steel gimbal joint on the 5m long torque steel arm in order to allow tilt and roll movements. The torque steel arm was mounted on the steel foundation via a swivel joint to allow movements in heave. The foundation with three steel legs and concrete feet were designed to stand firmly on the seabed, but to keep the main parts above the mud. The foundation had a horizontal flange on which a steel meteorology mast was mounted. The mast had three sections, two 3m sections and a top section with fitting for a sonic anemometer. The rotor tube was mounted with a measurement system to measure movements of the rotor tube. The turbine rotor was investigated for power and loads, and a modal analysis of structural dynamics was made both theoretically and experimentally, providing evidence for a structurally safe construction.

1. Introduction

This report describes development and manufacture of an experimental wind turbine, the DeepWind demonstrator. The purpose of this experimental wind turbine is to verify proof-of-principle of the DeepWind floating offshore vertical axis wind turbine concept, first described in 2009 [1]. The DeepWind concept is a floating vertical axis concept with a floating and rotating foundation. The concept gained a lot of support and EU funded the FP7 project DeepWind starting October 2011. This report describes design and manufacture of the DeepWind demonstrator 1kW wind turbine which is work package 7 of the EU project DeepWind. The report describes design philosophy, design specifications, analysis of test site, instrumentation, production of components, and structural dynamics testing. The design philosophy was discussed in the DeepWind consortium at the kick-off meeting November 2010, at the Delft meeting October 2011. There were two principally different design philosophies. The first philosophy was based on designing a 1kW wind turbine that fitted the test site in Roskilde fjord, and that would function properly according to the concept ideas. The other philosophy was based on designing a 1kW scaled down 5MW wind turbine that fitted the basin tests at Marin in Holland. The first design philosophy would fit free field experiments where wind, waves and sea currents occur randomly, and where high loads would be anticipated. The second design philosophy would fit the specific wind, wave and sea current configurations for a downscaled model of the 5MW machine, which would be designed as part of the project.

Different work packages of the project supported inputs to the design and construction of the DeepWind demonstrator. Work package 1 provided calculations of loads and power with the codes being developed to accomplish the DeepWind concept. Work package 2 provided design of the blades and rotor of the demonstrator. Work package 3 provided design and hardware of the generator and control system. Work package 4 and 5 provided only minor inputs to the demonstrator as the work of control system and mooring were made later in the project. Work package 6 provided valuable input of the Magnus forces on the rotor tube. This report describes the objectives of the experimental wind turbine, the design considerations, design criteria, design loads, manufacture, the test site, and initial testing of the demonstrator. The tests in Roskilde Fjord and at Marin are reported in other reports.

2. The DeepWind concept

2.1 Objectives of the DeepWind demonstrator

The main objective of building a demonstrator wind turbine is to verify that the DeepWind concept works. This means that it should be verified that the turbine is able to be installed at sea, and to be put in operation to produce power under the offshore conditions, without being jeopardized by severe dynamics and loads during operation. This includes the visual impression of the operation of the turbine. The second objective of the demonstrator is to demonstrate that the movements of the turbine under the conditions applied during the experiments can be verified by aeroelastic calculations. Aeroelastic codes to take account of the DeepWind design are developed in work packages 1 and 6.

The objectives of building the demonstrator is supplemented with the psychological effects of actually seeing the concept being materialized going through a design phase and to gain experimental experiences on the hardware under field conditions and under controlled conditions.

2.2 Design considerations

In the consortium it was discussed intensively whether to make a demonstrator for field conditions or a model for basin conditions, or to make both. The two philosophies of a demonstrator or a model are significantly diverging. The demonstrator for field conditions would be a robust construction optimized for a 1kW wind turbine, being built for adequate handling and for design loads that corresponds to the climate conditions at the test site. The model would be made as a scaled down turbine of a 5MW wind turbine using scaling laws for dimensioning the model [3] by a downscaling. The scale factors to be considered are shown in table 1.

Table 1 Summary of scale factors for model testing in offshore basin, re. Jonkman

Parameter	Unit	Scale Factor
Length	L	λ
Time	T	$\lambda^{0.5}$
Area	L^2	λ^2
Volume	L^3	λ^3
Mass	M	λ^3
Wave Celerity	LT^{-1}	$\lambda^{0.5}$
Wave Height	L	λ
Wave Period	T	$\lambda^{0.5}$
Wind Speed	LT^{-1}	$\lambda^{0.5}$
Wind or Wave Force	MLT^{-2}	λ^3
Power	ML^2T^{-3}	$\lambda^{7/2}$
Stress	$ML^{-1}T^{-2}$	λ
Modulusof Elasticity	$ML^{-1}T^{-2}$	λ
Modal Frequency	T^{-1}	$\lambda^{-0.5}$

The ideal situation would be to make both versions. However, the design of the 5MW turbine is made in work package 8 when all subcomponent studies have been finalized. The time scale of this work is not very well synchronized in order for a downscaling. A downscaled model based on initial guesses of a 5MW would not be satisfactory. It was therefore decided to use the demonstrator also for the basin measurements. This makes sense since the experiments in the completely different environments would supplement each other, and comparisons would be much easier. Relating the basin experiments to the 5MW design behaviour is, however, not possible. The relation between the 1kW demonstrator and the 5MW wind turbine must be made through the verification of the calculation codes. Besides that, the scaling factors in table 1 on geometric similarity do not satisfy the aerodynamic similarity parameter, the Reynolds number.

2.3 The initial DeepWind demonstrator setup design

The demonstrator concept is a floating vertical axis concept that potentially may be materialized in many different configurations with respect to how the generator is built into the construction,

how the safety system might be implemented, and how the torque might be absorbed [1]. The torque absorption system was further analysed and three different methods were described in [2]. Figure 1 shows the three torque absorption configurations. The first configuration has a generator fixed to the sea bed. In this case the rotor can move in tilt and roll but not in heave. In the second configuration the rotor can move in up and down in heave and the torque is absorbed in the torque arm. In the third configuration the rotor can furthermore move in translation. Among the three configurations the second was chosen due to the following reasons:

- The number of degrees of freedom is limited
- The configuration is practical with respect to installation and maintenance
- The configuration is will likely have lower tilt and roll than the third configuration

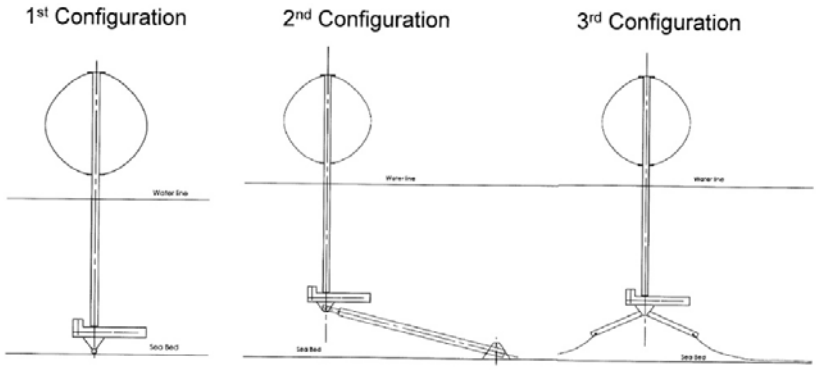

Figure 1 Mooring configurations for the DeepWind demonstrator

The initial demonstrator design setup should, apart from the wind turbine rotor, consider the conditions for installation and operation off the coast of Risø in Roskilde Fjord, and at the same time the demonstrator should be adaptable to the testing in Marin basin. The initial design setup for this purpose is shown in figure 2.

Figure 2 Initial DeepWind demonstrator test setup

2.4 The initial wind turbine rotor design

The rotor design was made by work package 1 partners. The depth at the test site in Roskilde Fjord is 5m, including half a meter of mud, while the depth at Marin basin is variable up to 10m. With these water depths it was found that a rotor of 2m diameter and 2m height would be adequate for a 1kW wind turbine. Some initial physical properties of the concept are shown in figure 3.

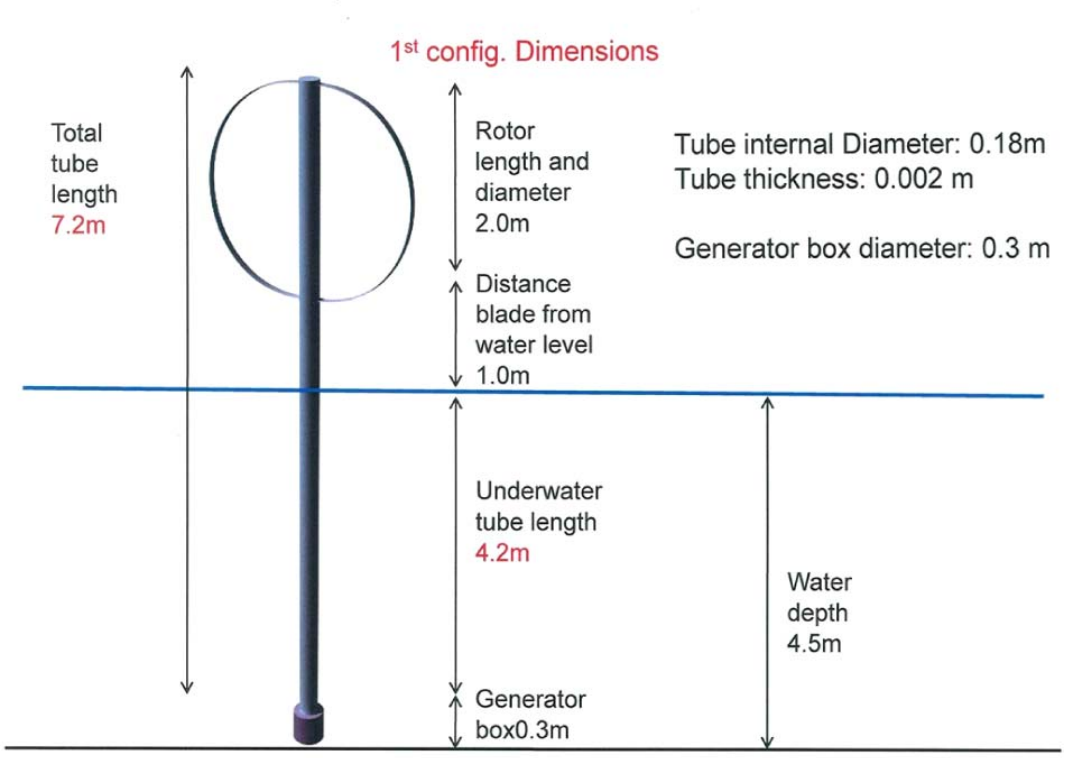

Figure 3 **First sketch of the demonstrator rotor with the overall dimensions**

Based on the initial physical properties the rotor was analysed for power, thrust and loads. Trento University provided aerodynamic calculations of the rotor [4]. Based on the classical Troposkien geometry, they made a parameter analysis where they varied the number of the blades, the rotor solidity, and the airfoil profile, see table 2.

The results of the analysis are shown in table 3 for a rated wind speed of 10m/s. They are calculated at the maximum power coefficient condition and they are considered more or less representative of the rated conditions, though following the control strategy at cut out wind speed the power and thrust could be 20-50% higher or more. The rated power is about 500-600W with a torque range between 10 and 16 Nm, depending on the rotor solidity. The streamwise thrust is about 100-130N and the transverse 10-30N. From the power point of view the rotor dimensions should be increased to have more power at rated wind speed and a better power coefficient (the latter would be also at lower wind speeds).

Table 2– Geometrical and working characteristics of the four wind turbines architectures analyzed

	A	B	C	D
Blade profile	NACA 0015	NACA 0018	NACA 0015	NACA 0018
Blade geometry	Troposkien configuration	Troposkien configuration	Troposkien configuration	Troposkien configuration
Number of blade	2	2	3	3
Height	2.0 m	2.0 m	2.0 m	2.0 m
Diameter	2.0 m	2.0 m	2.0 m	2.0 m
Chord	0.0858 m 0.1287 m 0.1716 m	0.0858 m 0.1287 m 0.1716 m	0.0572 m 0.0858 m 0.1144 m	0.0572 m 0.0858 m 0.1144 m
Solidity [= BcL/A_{sw}]	0.20 0.30 0.40	0.20 0.30 0.40	0.20 0.30 0.40	0.20 0.30 0.40

But also the thrust would increase, with the rotor weight and the thrust moment arm from the hinge at the seabed. The augmentation of the rotor dimensions should be carefully evaluated to ensure enough buoyancy force to sustain the structure. Also other considerations should be done if the same rotor will be tested in the water tank and in a wind tunnel.

Table 3 Comparison of aerodynamic power P and torque T, axial F_X and longitudinal F_Y thrusts between the different turbines at V_0 = 10 m/s and at $C_{P,MAX}$.

Solidity [BcL/A_{sw}]		**A (2-bladed NACA0015)**	**B (2-bladed NACA0018)**	**C (3-bladed NACA0015)**	**D (3-bladed NACA0018)**
0.20 0.30 0.40	**tsr [-] (□ [rpm])**	5.00 (334) 4.25 (284) 3.75 (251)	4.75 (318) 4.25 (284) 3.75 (251)	5.00 (334) 4.25 (284) 3.75 (251)	4.50 (301) 4.25 (284) 3.75 (251)
0.20 0.30 0.40	**$C_{P,MAX}$ [-]**	0.3296 0.3658 0.3808	0.3260 0.3699 0.3866	0.3235 0.3633 0.3797	0.3015 0.3493 0.3743
0.20 0.30 0.40	**P_{MAX} [kW]**	0.5138 0.5702 0.5936	0.5081 0.5766 0.6027	0.5043 0.5664 0.5920	0.4700 0.5445 0.5835
0.20 0.30 0.40	**T_{MAX} [Nm]**	10.2760 13.4166 15.8301	10.6979 13.5683 16.0733	10.0851 13.3270 15.7853	9.8944 12.8123 15.5606
0.20 0.30 0.40	**F_X [N]**	103.3680 117.7669 125.5352	103.8418 119.3043 126.3152	103.2241 117.9260 126.3565	107.5970 123.4954 129.7188
0.20 0.30 0.40	**F_Y [N]**	-14.0069 -22.0119 -29.0531	-13.5551 -21.0433 -27.9692	-12.0462 -19.6393 -26.9057	-13.9675 -20.5078 -26.7749

If the same chord length should be selected for the two and three-bladed rotor due to mould cost, it would be preferably in the range of 0.095m to 0.107m. This leads to a rotor solidity of 0.22 (B = 2) and 0.33 (B = 3) for the smaller chord and 0.25 (B = 2) and 0.37 (B = 3) for the bigger one. Once selected the rotor dimension (2m height and 2m diameter), the maximum expected shaft power at a rated wind speed of 10m/s is almost 600W and the nominal torque range is between 11Nm and 15Nm, but at higher wind speeds they could be higher depending on the control logic.

The increase of the rotor dimensions (diameter and height) from the current 2.0m up to a maximum of 2.5m could be taken into consideration to improve the power at rated condition and the aerodynamic performance for all the conditions, but it should be carefully evaluated due to the limited available buoyancy force and the restrictions for the wind tunnel and water tank tests.

In the following tables 4-6 the principal results for the different rotor configurations are summarized.

Table 4 Possible final rotor geometric configurations.

Rotor Config.	Height [m]	Diameter [m]	Solidity	Number of blades	Chord [m]	Airfoil
A	2	2	0.22	2	0.095	NACA 0015-0018
B	2	2	0.25	2	0.107	NACA 0015-0018
C	2	2	0.33	3	0.095	NACA 0015-0018
D	2	2	0.37	3	0.107	NACA 0015-0018

Table 5 Functional parameters for the different rotor configurations with the NACA0015 profile at design conditions (V = 7m/s, max C_P).

Rotor Config.	λ_{design}	ω_{design} [rpm]	$C_{P,design}$	ω_{range} [rpm] (4-10m/s)	Re_{design} min-max
A	4.75	318	0.327	182-454	$1.71\text{-}2.59*10^5$
B	4.50	301	0.338	172-454	$1.80\text{-}2.78*10^5$
C	4.25	284	0.356	162-406	$1.49\text{-}2.36*10^5$
D	4.00	267	0.364	153-382	$1.55\text{-}2.52*10^5$

Table 6 Power, torque and forces for the different rotor configurations with the NACA0015 profile at rated conditions (V = 10m/s, max C_P).

Rotor Config	P_{rated} [W] (ω [rpm])	$T_{rated,ave}$ (min-max) [Nm]	$F_{x,rated,ave}$ (min-max) [N]	$F_{y,rated,ave}$ (min-max) [N]
A	530 (454)	11.2 (-2.7 - 20.8)	106.3 (2.1 – 189.9)	-15.7 (-136.3 – 100.2)
B	547 (454)	11.5 (-2.9 – 21.4)	114.4 (2.3 – 203.1)	-18.5 (-148.9 – 107.6)
C	577 (406)	13.6 (10.8 – 16.9)	124.6 (107.2 – 142.2)	-22.6 (-43.4 – 2.7)
D	588 (382)	14.7 (12.0 – 18.1)	127.3 (109.7 – 145.6)	-25.6 (-48.0 – 2.4)

2.5 The initial DeepWind demonstrator design

The initial demonstrator design was analysed by Vita and reported in [6]. He later updated and renamed the report, see [9]. He simulated the loads and movements of a 2-bladed Darrieus rotor configuration with the aeroelastic HAWC2 code. The study included the loads from aerodynamics, hydrodynamic lateral force and waves. The analysis was based on coordinate systems setup as shown in figure 4. The suffix G refers to the global reference system, gb to the generator box reference system, T to the tower reference system, B the blade reference system, L the local reference system on the blade, and W the wind reference system.

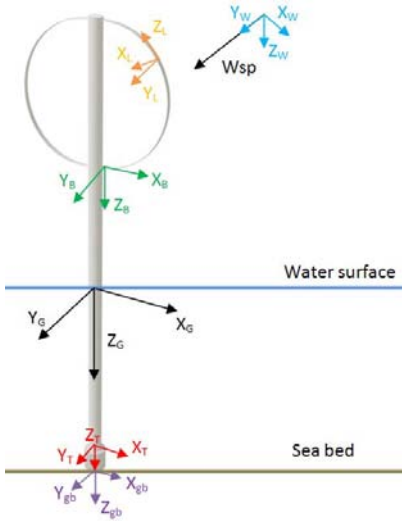

Figure 4 Coordinate system used in the analysis of the demonstrator

The analysis was made on two different blade profiles, NACA0018 and the TU Delft profile DU06-W-200 with a chord of 0.172m. The Aluminium rotor tube was 5m long, with an external diameter of 0.17m and a thickness of 2mm.

The analysis was made for two configurations, a land configuration that only considered the rotor without hydrodynamic loads, and an offshore configuration that considered all loads. The land configuration of the rotor is shown in table 7 and of the tube in table 8.

Table 7 Rotor geometry, from last DeepWind report

ROTOR GEOMETRY		
Blade profile	NACA	TU20
Blade geometry	Troposkien	Troposkien
N	2	2
H [m]	2.0	2.0
R [m]	1.0	1.0
c [m]	0.172	0.172
σ	0.4	0.4

The geometry of the tower is summarized in the table below.

Table 8 Rotor tube data

	Land Configuration
H [m]	2
H_0 [m]	0.5
H_w [m]	/
Htot [m]	2.5
R_T [m]	0.85
Th [m]	0.002
Material	Al
Hg [m]	0.3

2.5.1 Modal analysis of land configuration

For the land configuration a modal analysis was made where the natural frequencies of the rotor were determined, as shown in table 9 and figure 5.

Table 9 First ten vibration modes and natural frequencies (rotor fixed at bottom)

	Mode shape	Natural frequency (Hz)
Mode 1	1st tower out of plane	15.79
Mode 2	1st tower in plane	16.75
Mode 3	1st blade flapwise symmetric	25.04
Mode 4	1st blade flapwise antisymmetric	25.61
Mode 5	1st rotor twist	26.83
Mode 6	1st blade edgewise	28.04
Mode 7	2nd rotor twist	35.52
Mode 8	2nd tower out of plane	36.51
Mode 9	3rd tower out of plane	38.84
Mode 10	3rd rotor twist	40.62

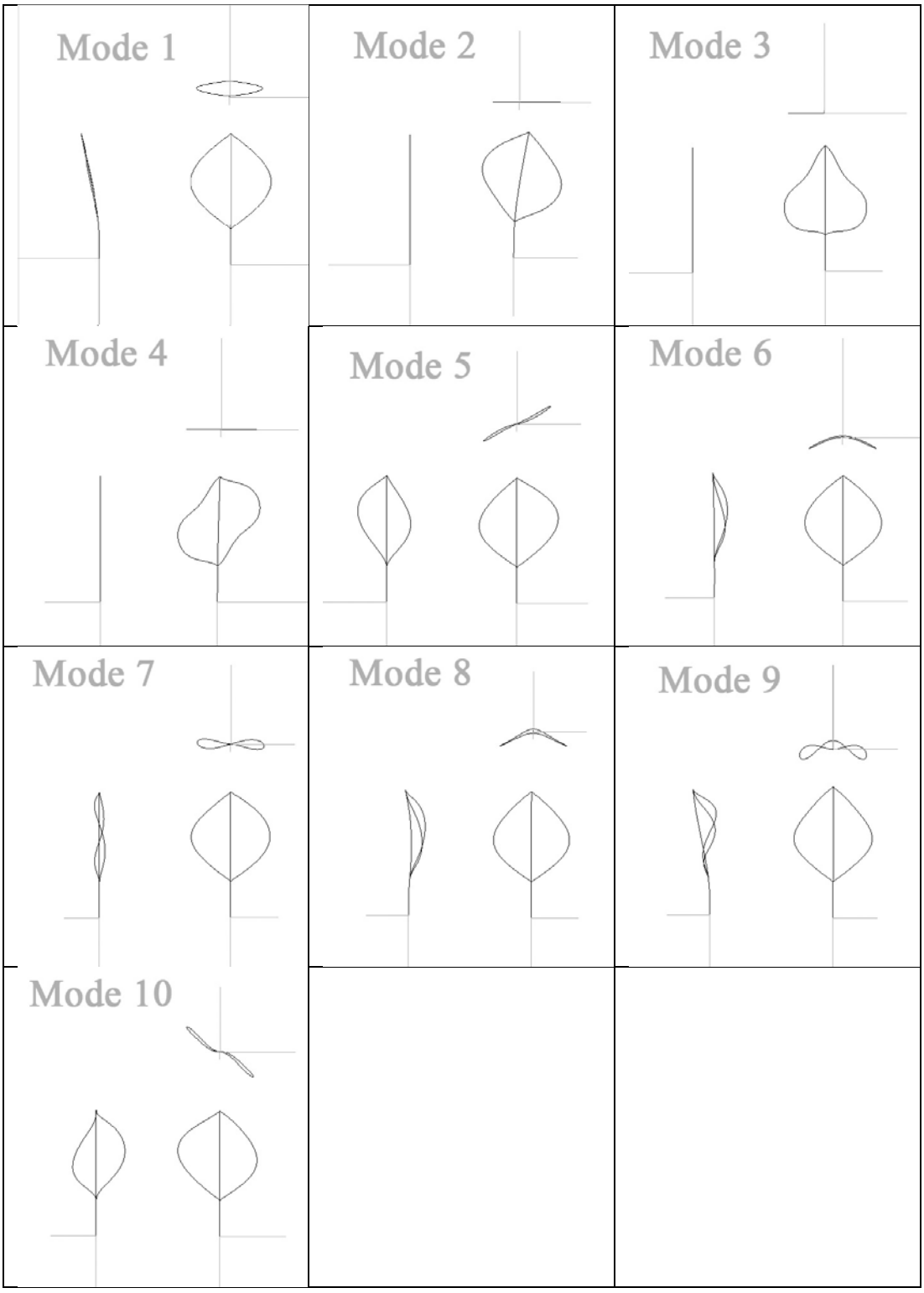

Figure 5 The first ten modes of vibration and natural frequencies of the demonstrator turbine

2.5.2 Time domain simulations on land configuration

The land simulations with HAWC2 were made in time domain. The “measurement” points for the loads are shown in figure 6.

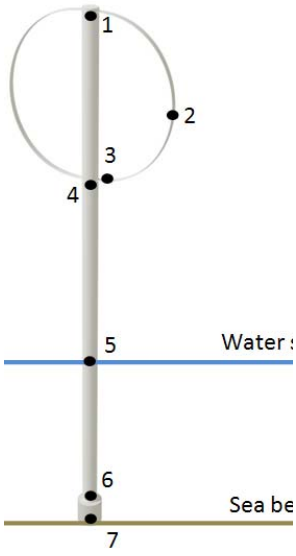

Points N.	Body	Position on the body
1	Tower	top
2	Blade	centre root
3	Blade	lower root
4	Tower	blades connection
5	Tower	mean water level
6	Tower	bottom
7	Generator box	bottom

Figure 6 Position of the measurements points, dimensions are not indicative of the real design.

There was carried out 11 simulations on the land configuration as shown in table 10.

Table 10 Simulations carried out for land configuration

Simulation N.	Wsp [m/s]	Profile	ω_r [rpm]	Frequency acquisition data [Hz]
0	No wind	NACA	0-500	75
1	7 constant	NACA	251	75
2	7 constant	Tu20	251	75
3	10 constant	NACA	358	75
4	10 constant	Tu20	358	125
5	12.3 constant	NACA	440	125
6	12.3 constant	Tu20	440	125
7	16 constant	NACA	410	75
8	16 constant	Tu20	410	75
9	4–16 variable	NACA	varies with wsp	20
10	4–16 variable	Tu20	varies with wsp	20

Variable wind speed and rotational speed simulation

Here the long run with Tu20 airfoils and with increasing wind speed from 4 to 16 m/s is shown, The rotational speed is regulated as shown in Figure 7. The values of ω_r are taken from the aerodynamic reports of Trento [4,5]. For wind speed lower than 4m/s the rotational speed is kept constant at 143rpm. In the wind speed range from 4m/s to 12.3m/s the rotational speed increases linearly with the wind speed. At 12.3m/s, the turbine reaches its maximum rotational speed, i.e. 441rpm. ω_r is kept constant until 12.5m/s. In the range from 12.5m/s to 16m/s the rotational speed is reduced up to 350rpm. At wind speed higher than 16m/s the turbine is stopped, see table 11. The rotor to generator gearing ratio is 1:4.788.

Table 11 Rotational speed and rotational frequency at different wind speeds

Wind speed [m/s]	ω_r rotor [rpm]	ω_n generator[rpm]	f_{1p} [Hz]
0 – 4	143.24	685.83	2.38
4 – 12.3	143.24 – 441.17 (linearly increased)	685.83 – 2112.36	2.38 – 7.35
12.3 – 14	441.17	2112.36	7.35
14 – 16	441.17 – 340.0 (linearly decreased)	2112.36 – 1627	7.35 - 5.67

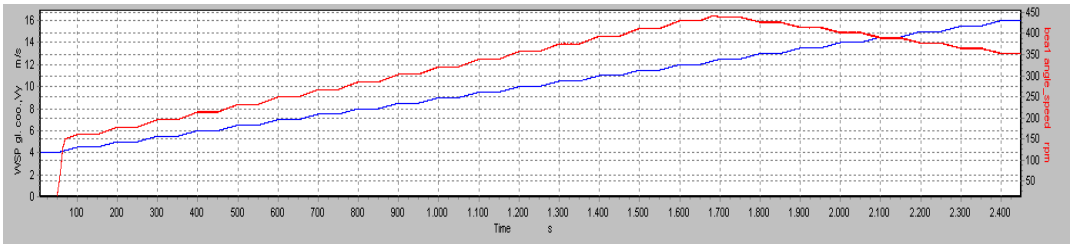

Figure 7 Simulation 10, rotational speed ω_r in red and wind speed w_{sp} in blue

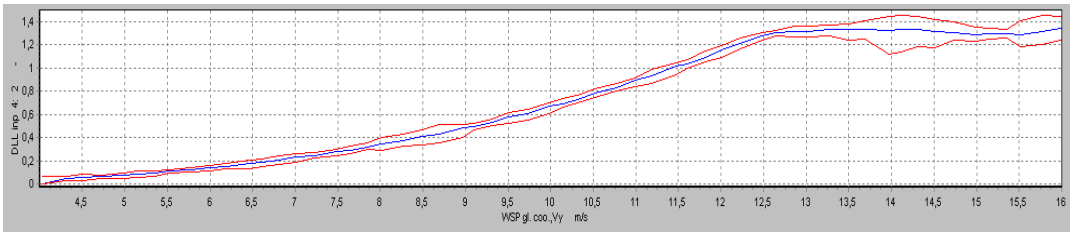

Figure 8 Simulation10, Power curve, mean value (blue) and deviations (red)

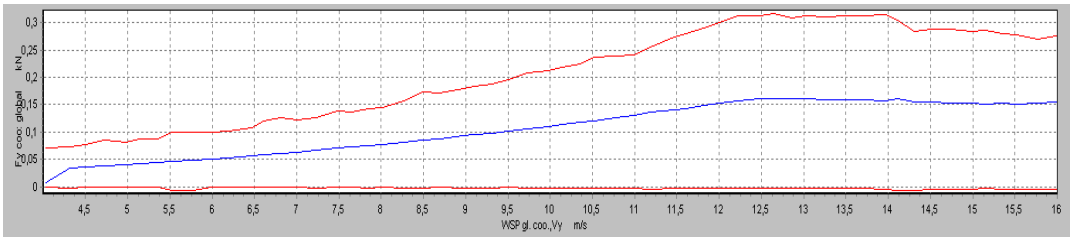

Figure 9 Simulation10, Fy measured at low root height (point4 in fig 6). Mean value (blue) and max – min (red).

The rotational speeds and wind speeds are shown in figure 7. The power as function of wind speed is shown in figure 8, and the thrust F_y is shown in figure 9.

Constant wind speed simulations

The simulations at constant wind speed give more reliable results, because of a lower time step. For the constant wind speed simulations the loads on the turbine in different operational points were analysed. Table 12 shows the calculated values of the power P and the torque Q for the eight simulations 1-8 in table 10.

Table 12 Power and torque on the shaft, on land simulations

POWER / TORQUE OUTPUT								
	Sim. 1	Sim. 2	Sim. 3	Sim. 4	Sim. 5	Sim. 6	Sim. 7	Sim. 8
P [kW]	.198	.214	.575	.617	1.05	1.12	1.07	1.16
Q [Nm]	7.67	8.30	15.73	16.9	23.82	25.41	24.10	28.23

Figure 10110 to 12 show the results for simulation 1. These results are comparable to the cases investigated by Trento University [5]. The loads are calculated in the global reference system (Figure 101) and in the tower reference system (Figure).

The forces on the tower in point 4 for the simulations 1-8 are shown in table 13. The bending moments on the tower at the cross section 0.5 meter below the blades are shown in table 14. This point corresponds to the mean water level in the offshore configuration, point 5 in Figure 6. The loads on the blades in two points: at the centre of the blade, point 2, and at the lower root point 3 in figure 6,.are shown in table 15. The tower accelerations at the tower top and at the mean sea level are shown in table 16.

The data in table 12 reveal that the blade profile Tu20 performs better than the NACA profile. In terms of power output it is 6.6% higher at rated wind speed (12.3m/s) and 7.4% higher at design wind speed (7m/s)..

The values of the simulations with the NACA profile, in particular in simulation1, seem quite consistent with the data provided by Trento [5]. The HAWC2 values are slightly lower.

The plots of the loads on the tower (point 4), in different reference systems, offer the following observations:

- From figure 10 (global reference system):
  As expected, Fy has a positive mean value and the minimum is around zero. Fx has a negative mean value, quite close to zero. The frequency of the loads is f_{2p}.
- From figure 11 (tower reference system):
  Both Fx and Fy have mean values close to zero. The period of the loads is f_{1p}. The longitudinal load has also another characteristic period around 34Hz (figure 12). This is probably due to one of the higher modes of the tower out of the plane (around the x axis), perhaps it is f= mode9 -1p. It is an interesting result, because it shows that higher modes can be relevant at high rotational speeds.

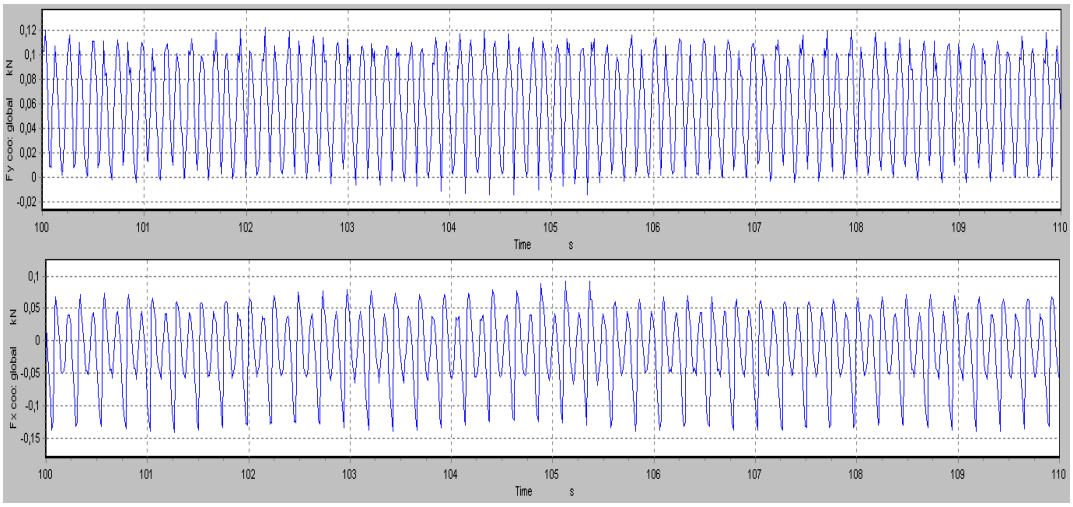

Figure 101 Simulation1, from top: Thrust Fy, transverse load Fx on the tower (point 4, fig 6), Global reference system

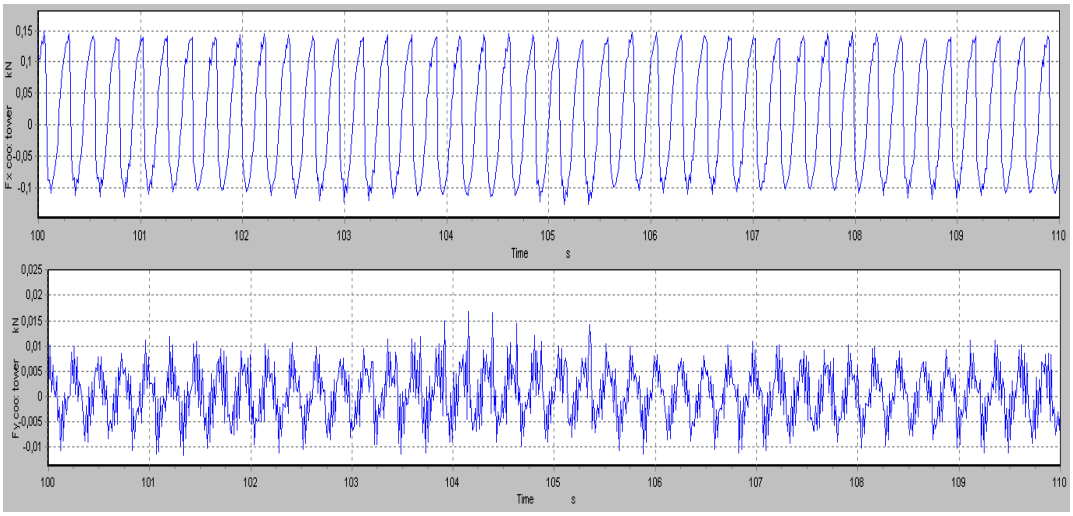

Figure 11 Simulation1, from top: transverse load Fx, thrust Fy on the tower (point 4, fig 6), Tower reference system

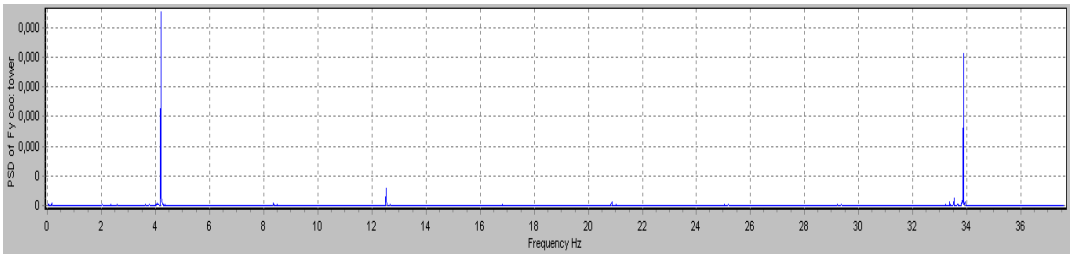

Figure 12 Simulation1, Power spectrum of thrust Fy on the tower (point 4, fig 6), Tower reference system

Table 13 Forces on the tower – on land configurations (Max / Min values). Global and tower reference systems.

FORCES ON THE TOWER - Point 4								
	Sim. 1	Sim. 2	Sim. 3	Sim. 4	Sim. 5	Sim. 6	Sim. 7	Sim. 8
Fx (g.r.s.) [N]	91.1	89.9	118.9	129.1	169	170.2	211.8	190.1
	-139.6	-141.0	-171.8	-166.7	- 213	-208.1	-242.0	-206.6
Fy (g.r.s.) [N]	121.8	128.6	202.9	205.6	286.8	303.8	289.8	295.1
	-25.1	-.8.2	-34.0	-2.2	-28.1	-10.1	-78.0	-34.1
Fx (t.r.s.) [N]	147.9	148.5	206.4	212.2	288.3	305.9	309.2	305.5
	-126.3	-130.4	-200.0	-206.1	-288.0	299.3	-304.0	283.9
Fy (t.r.s.) [N]	16.7	16.6	30.1	25.2	27.3	34.5	32.2	37.6
	-11.6	-16.8	-26.1	-25.2	-27.1	-31.7	-29.7	-38.1

Table 14 Moment on the tower, point 5 – on land configurations (Max / Min values).

MOMENTS ON THE TOWER – Point 5 (g.r.s.)								
	Sim. 1	Sim. 2	Sim. 3	Sim. 4	Sim. 5	Sim. 6	Sim. 7	Sim. 8
Mx [Nm]	234.9	245.6	290.9	310.2	427.6	416.6	427.2	410.4
	-79.5	-38.4	-57.8	6.0	-92.8	-12.45	-92.5	-16.0
My [Nm]	338.9	335.8	346.3	324.9	423.5	393.9	425.9	400.7
	-209.1	-164.9	-227.4	-263.6	-305.7	-253.3	-306.6	-329.3

Table 15 Loads on the blades, points 2 and 3 – on land configuration (Max / Min values)

LOADS ON THE BLADES (l.r.s.)								
	Sim. 1	Sim. 2	Sim. 3	Sim. 4	Sim. 5	Sim. 6	Sim. 7	Sim. 8
Fx [N]	-70.6	-70.9	-133.3	-160.2	-196.4	-198.9	-163.8	-223.5
(point3)	-78.0	-79.2	-146.8	-174.6	-218.3	-220.3	-194.9	-244.7
Fy [N]	7.87	8.96	10.47	11.2	21.9	17.15	16.8	15.2
(point3)	-3.85	-3.67	-1.48	0.01	-6.8	0.43	3.2	0.80
Fz [N]	474.4	480.7	984.3	$1.18\ 10^3$	$1.45\ 10^3$	$1.52\ 10^3$	$1.31\ 10^3$	$1.64\ 10^3$
(point3)	417.0	419.8	864.6	$1.05\ 10^3$	$1.32\ 10^3$	$1.33\ 10^3$	$1.10\ 10^3$	$1.50\ 10^3$
Mx [Nm]	-1.49	-1.7	-4.1	-4.56	-5.7	-7.3	-7.79	-7.55
(Point3)	-2.84	-3.14	-4.9	-5.52	-8.1	-8.46	-9.14	-9.00
My [Nm]	-16.4	-16.36	-30.8	-36.79	-45.4	-45.8	-38.5	-51.4

(Point3)	-17.7	-17.96	-32.8	-38.99	-48.8	-49.1	-43.6	-54.8
Mz [Nm]	4.89	5.18	2.14	2.33	9.77	3.60	3.17	2.1
(Point3)	-5.91	-6.23	-4.13	-4.62	-11.3	-6.85	-6.65	-5.2
Fx [N]	15.39	15.36	28.4	35.9	41.8	41.59	61.9	46.7
(point2)	14.32	14.30	26.7	31.4	39.1	39.62	36.4	43.2
Fy [N]	3.73	3.90	1.39	1.46	6.74	2.28	4.56	1.21
(Point2)	-2.93	-3.19	-0.91	-0.84	-5.70	-1.17	-4.15	-0.04
Fz [N]	162.7	169.5	333.6	397.1	506.1	537.5	456.9	569.6
(Point2)	101.0	103.7	204.6	260.5	310.8	320.5	224.6	369.1

Table 16 Accelerations at tower top, point 1 – on land configuration. (Max /Min values). Gravitational contribution is not included

TOWER ACCELERATIONS – Point 1 (g.r.s.)								
	Sim. 1	Sim. 2	Sim. 3	Sim. 4	Sim. 5	Sim. 6	Sim. 7	Sim. 8
a_{xT} [m/s^2]	3.78	3.68	4.87	1.84	11.02	8.80	8.62	2.15
	-3.71	-3.59	-4.12	-0.99	-8.30	-5.71	-5.33	-1.39
a_{yT} [m/s^2]	3.26	3.27	3.63	1.71	8.33	4.61	4.59	1.68
	-3.18	-3.09	-2.77	-1.85	-5.81	-2.98	-2.47	-1.79
a_{zT} [m/s^2]	0.033	0.035	0.041	0.009	0.071	0.065	0.062	0.014
	-0.029	-0.029	-0.038	-0.008	-0.066	-0.058	-0.058	-0.013

2.5.3 Simulations on offshore configuration

Test site conditions at Roskilde Fjord

The turbine will be placed at Roskilde fjord close to the Risø marina pier.

Assuming a water depth of 5m and a wind speed of 20m/s, DHI estimated the following characteristics for the site [8]:

- H_S, significant wave height, is 0.9m.
- T_P, peak period of the wave spectrum, is 3.2s, corresponding to f_P=0.31Hz.
- The currents are expected to have a vertical averaged speed of 0.1m/s, as maximum value. The relative Re (on the tower diameter) is 1.2 10^4.

Due to the uncertainty of the water depth, a conservative value of 4m is assumed.

For fixed circular frequency of the wave spectrum ω_P, the wave spectrum is calculated with the JONSWAP model (using a shape factor of 1.25). Most of the wave energy is concentrated in waves of period between:

$$1.05s<T_w<4.25s,$$

Corresponding to:

$$0.23\text{Hz}\ (1.47\ \text{radians/s}) < f_w < 0.95\text{Hz}\ (5.98\ \text{radians/s}) \quad (1)$$

Given H_S, it is also possible to estimate the value of the extreme wave height]:
$H_{2\%}$=1.4 H_S= 1.26m.

Other characteristic parameters are calculated using linear wave theory. A list of the wave characteristic numbers expected at the test site at Roskilde fjord, is shown in table 17.

Table 17 Characteristic numbers for the waves at the site

	Infinite water depth	Correction for finite depth
ζ_a (wave amplitude) [m]	0.45	.45
λ_w (wavelength) [m]	16.11	14.92/15.01
T_p [s]	3.2	3.2
f_p [Hz]	0.31	0.31
ω_p [rad/sec]	1.96	1.96
K (wave number) [1/m]	0.39	0.42
H_s [m]	0.9	0.9
$H_{2\%}$ [m]	1.26	1.26
h [m]	4	4

Design constraints and first iteration values

The turbine tests in the fjord were supposed to be tested under three possible configurations, see figure 1. Due to the limited space to design the underwater tower it was only considered to simulate on the third configuration which have the highest numbers of degrees of freedom. Due to the wave height, the mooring lines have to be at least 1m long. Then the underwater structure has a length of 3m. The generator box was intially estimated to be 0.3 x 0.3m.
The length of the underwater part of the tube is then 2.7m.
The rotor clearance from the mean water level is 0.5m. This value is very close to the wave amplitude, but it is has been chosen based on the following considerations:

- The turbine is supposed to be stopped in case of extreme conditions
- The lower root of the blades have a low speed, this may avoid major damages in case a wave would hit a blade
- The design needs the rotor to be as lighter as possible.

The first design parameters are summarized in figure 13.

The first design characteristics of the turbine were then obtained as shown in figure 14.

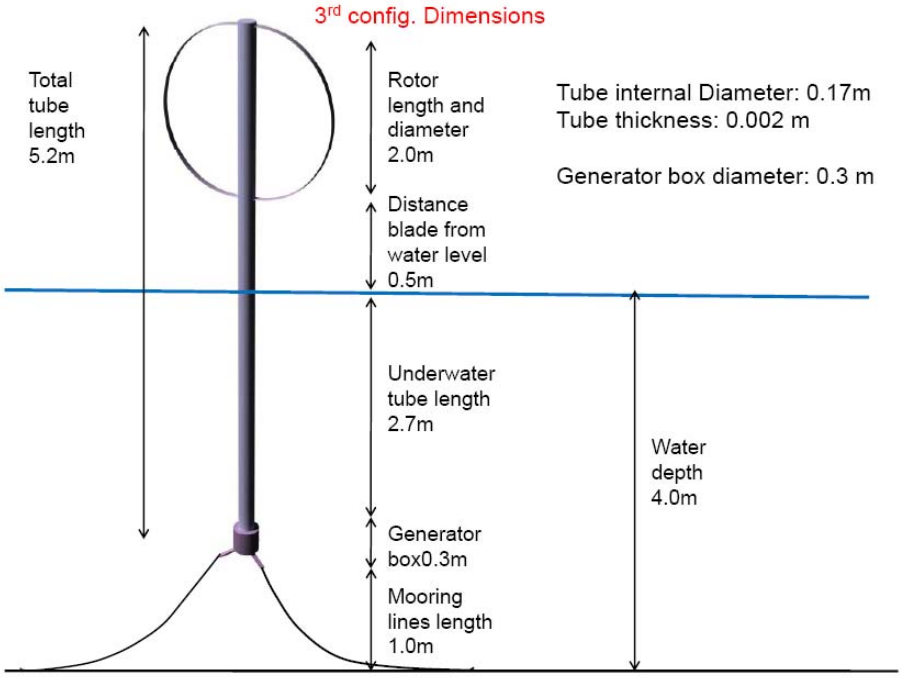

Figure 13 Design parameters

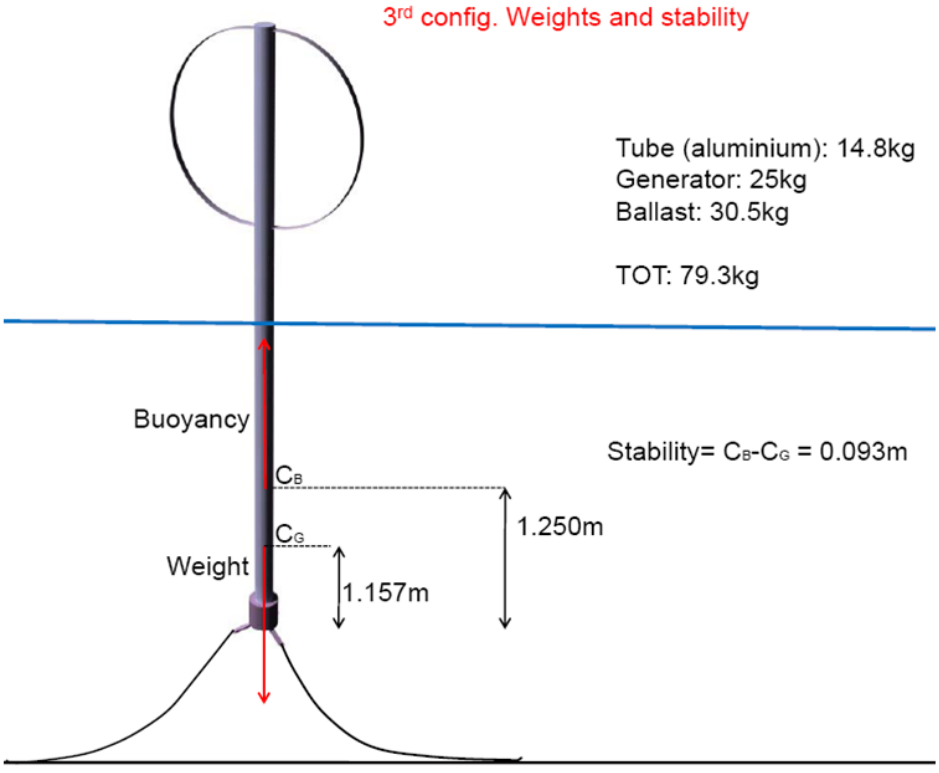

Figure 14 First iteration design

Design of the spar floating tower

The design of a spar buoy system has been fully studied and described in literature in the past years for large floating structures. Some literature exists also on small spar buoys, used for experiments, such as wave measurements. Such a floating system has six degrees of freedom, three rotational and three translational, as shown in figure 15 and summarized in table 18. For a correct design, equilibrium is necessary in all the six modes.

Table 18 Degrees of freedom of a floating system

Index	DOF	Displacement	Critical for spar system
1	Surge	η_1 ,translation on the x axis, [m]	No
2	Sway	η_2 ,translation on the y axis, [m]	No
3	Heave	η_3 ,translation on the z axis, [m]	Yes
4	Roll	η_4 ,translation around the y axis, [degrees]	Yes
5	Pitch	η_5 ,translation around the x axis, [degrees]	Yes
6	Yaw	η_6 ,translation around the z axis, [degrees]	No

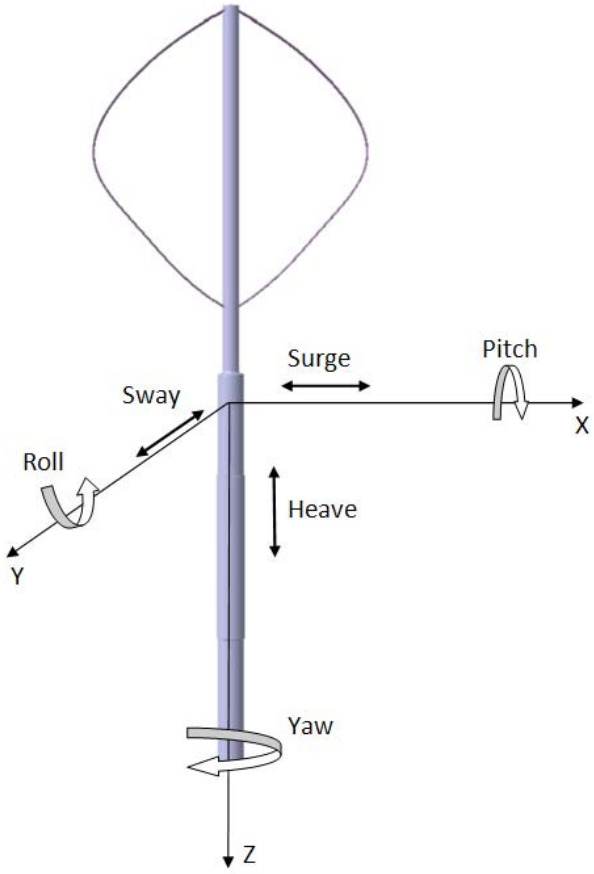

Figure 15 Degrees of freedom of a floating spar buoy system

The most critical motions for a spar buoy platform are the heave and the pitch (the roll is considered equivalent for symmetrical considerations). In this initial design phase, a steady-state design optimization is carried out. The design is based on these conditions:

1. Vertical equilibrium in heave

2. Equilibrium of the pitch moment, at the maximum values of the aerodynamic, hydrodynamic and wave loads.
3. Verification of the natural periods in heave and pitch, in order to avoid resonance frequencies.

The mathematical formulation of the steady state design optimization is described by Vita in [9] and is not further explained here.

The calculations lead to a modification of the offshore design as shown in table 19.

Table 19 Modified design. In red the parameters determined by external conditions or by the design of other components

Length Mooring lines [m]	1
Generator box diameter and height [m]	0.3 x 0.3
H_w [m]	2.7
H_{TOT}	5.2
R_T [m]	.13
Radius distribution (underwater)	Constant
Weight 1 blade [kg]	3.0
Weight tower (H_{TOT}) [kg]	20.46
Ballast + Generator weight [kg]	138
W_{TOT} [kg]	164.46
B	164.55

The dimension of the tower is still small compared to the wavelength, being $D/\lambda=0.017<0.2$. The drag force on the tower has been recalculated and shown along with Cd in figure 18.

The new coefficients, describing the stability of the system, are listed in table 20.

Table 20 Offshore coefficients for the determination of the stability of the turbine (positions in g.r.s.)

Z_G [m]	2.40
Z_B [m]	1.54
Z_G-Z_B [m]	0.86
C_{55} [kg m^2/s^2]	1392.87
T_{n3} [s]	6.41
ω_{n3} [Hz]	0.15
T_{n5} [s]	5.68
ω_{n4} [Hz]	0.17
η_3 [m] (from wave loads)	.065 cos(1.69t)
η_5 [deg] (from wave loads)	5.18 sin(1.69t)
η_5 [deg] (from aerodynamic and hydrodynamic constant load)	19.63
η_5 [deg] (from aerodynamic periodical terms)	0.009 cos(48.33t)

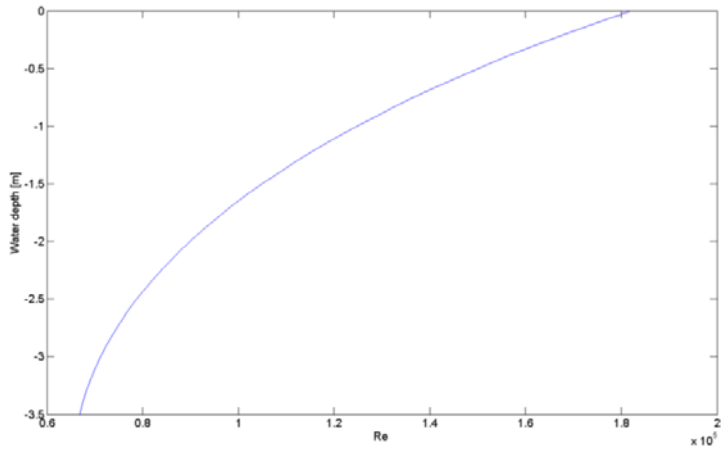

Figure 16Range of oscillatory Reynolds numbers for the demonstrator, modified design.

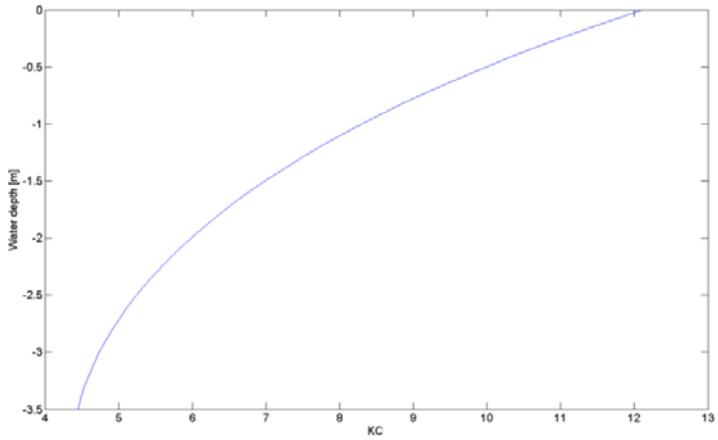

Figure 17 Range of KC numbers for the demonstrator, modified design.

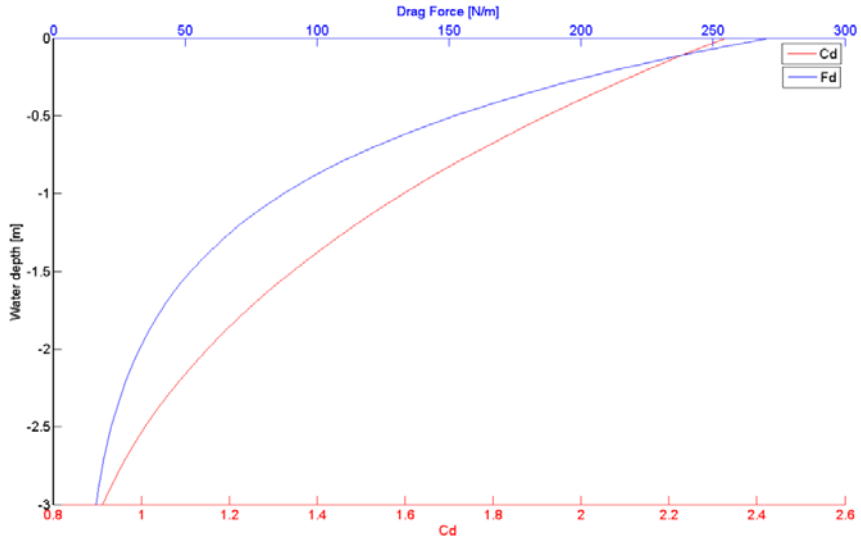

Figure 18 Cd and Fd for the demonstrator, modified design.

The amplitude of the heave motion is decreased almost 50%, obtained by adding the ballast on the bottom. The turbine is now in equilibrium in pitch, even though the maximum pitch angle is considerable, i.e. ϕ=19.63 + 5.18cos(1.96) deg. However it should be noticed that these values have been obtained under conservative conditions. Moreover at maximum wave loads, the turbine is supposed to be not operative. Therefore, the two situations of max wave loads and max aerodynamic loads should not happen at the same time.

As expected, the strong variation of the aerodynamic loads doesn't seem to influence on the equilibrium of the floating turbine.

2.5.4 Offshore simulations

Code set up

The offshore simulations of the turbine were made for configuration 1 of figure 1. In this configuration the spar buoy floats, and the torque is absorbed through torque arms that are connected to the sea bed with anchor chains.

The rotor and aerodynamic set up is the same used for the on land calculations. The blade profile is the Tu20, that performed better in the previous simulations. Waves and currents are generated to simulate the offshore environment.

There were carried out 11 simulations combining:

- Wind speed, constant of 7m/s and 12.3 m/s
- Waves of amplitude .4m and period 2s.
  The wave directions, β_w, are 0 and 90 degrees, referred to the wind speed direction.
- Water current of maximum speed 0.1m/s. The current has a power law profile with coefficient 0.5.
  The directions β_c of the current are 0 and 90 degrees, referred to the wind speed direction.

The complete list of the simulations is reported in table 21.

Table 21 Simulations for the offshore configuration

Sim. N.	Wsp [m/s]	ϕ_0 [deg]	H_s [m]	T_P [s]	β_w [deg]	β_c [deg]	U [m/s]	ω_r [rpm]
11	No aerodynamics	5	-	-	-	-	-	0
12	No aerodynamics	5	-	-	-	-	-	0 - 350
13	7 constant	0	-	-	-	-	-	251
14	12.3 constant	0	-	-	-	-	-	440
15	7 constant	0	0.45	2	90	-	-	251
16	12.3 constant	0	0.45	2	90	-	-	251
17	7 constant	0	0.45	2	0	-	-	440
18	12.3 constant	0	0.45	2	0	-	-	440

19	7 constant	0	0.45	2	0	0	0.1	251
20	12.3 constant	0	0.45	2	0	0	0.1	440
21	12.3 constant	0	0.45	2	0	90	0.1	440

Natural frequency verification

The first two offshore simulations, 11 and 12, do not include aerodynamic loads. These two simulations were carried out in order to verify the inertial behaviour of the turbine and its natural frequencies in pitch and roll. The results are shown in terms of surge dx, sway dy and heave dz, displacements of the cross sectional area of the tower at the mean water level.

In simulation 11, the turbine is tilted 5 degrees off the x axis, and it is left free to oscillate in the water. In figure 19 the time series of dx and dy are plotted.
The results show:

- The natural period in pitch and roll are equal and close to 6s, as expected.
- The pitch motion generates also a roll motion, even though of small amplitude. This is caused by gyroscopic coupling.
- The pitch motion is quite well damped

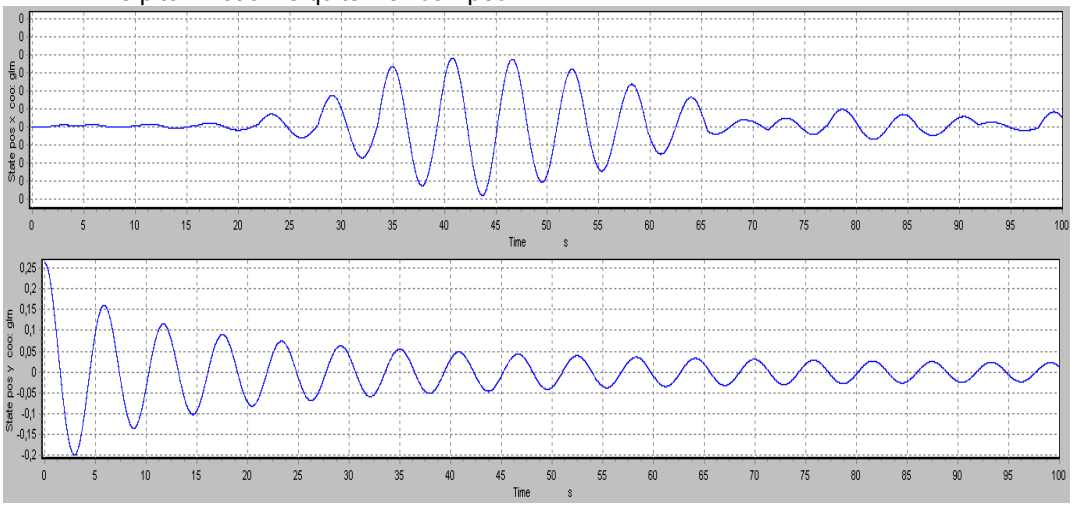

Figure 19Simulation 11 - From top: surge dx and sway dy at the water level

In simulation 12, the turbine is also spinning up to 350rpm. In figure 20 surge, dx, sway dy and heave dz are plotted along with ω_r. The plots allow some observations:

- The natural periods are strongly affected by the rotational speed. At 350rpm, the period of the oscillations is greater than 40s. The same effect is present in both pitch and roll.
- dz, shows a very stiff behaviour of the turbine
- As expected, at lower rotational speed some high frequency effects are visible. At high rotational speed, the inertia cancels those effects and the plot appears to be smoother.
- The roll motion generated by the pitch, it has a low amplitude, but also a low damping.

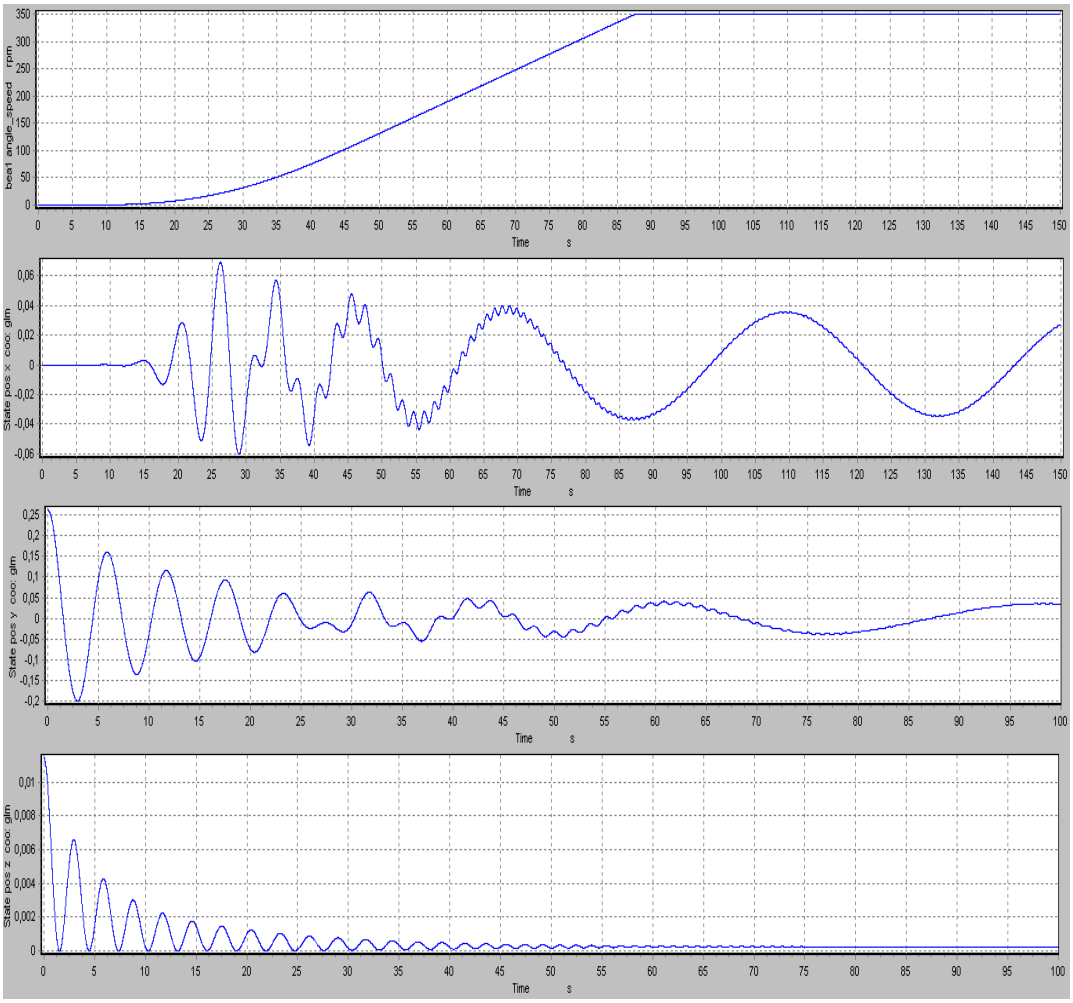

Figure 20 Simulation 12, from the top: 1.rotational angular speed ω_r, 2. Surge dx, 3.sway dy, 4.heave dz.

2.5.5 Results from simulations

In this section the results are reported, but they are limited to the most significant results for the setup of the offshore configurations:

- Parameters to evaluate the stability of the turbine: ϕ_{mean}, ϕ_{max} (table 22). These values don't include the deflection of the tower.
- Parameters to choose the instrumentation for the test: a_{xT}, a_{yT}, a_{zT} at the mean water level (point5) and at the tower top (point1), table 23
- Loads in offshore environment: Mx and My on the mean water level cross section of the tower (point 5), table 24

Along with the data reported in the tables, some time series of the tilt angle are plotted in figures 21-23.

Table 22 Tilt angle of the turbine (tower deflection not included)

TOWER STABILITY (g.r.s.)									
	Sim. 13	Sim. 14	Sim. 15	Sim. 16	Sim. 17	Sim. 18	Sim. 19	Sim. 20	Sim. 21
ϕ_{mean} [grad]	9.28	17.07	11.39	17.18	11.43	18.68	11.38	18.73	17.34
ϕ_{max} [grad]	16.31	23.38	17.85	20.18	18.12	22.42	17.89	22.50	20.11

Table 23 Aceleration on the tower – offshore configuration (gravity not included)

TOWER ACCELERATIONS (g.r.s.)							
	Sim. 15	Sim. 16	Sim. 17	Sim. 18	Sim. 19	Sim. 20	Sim. 21
ax_T [m/s^2] (Point1)	14.48 -7.42	22.56 -10.35	14.39 -7.42	11.81 -6.47	14.45 -7.36	11.93 -6.25	22.65 -10.14
ay_T [m/s^2] (Point1)	9.21 -6.07	12.73 -10.27	9.23 -6.07	7.39 -5.88	9.29 -6.26	7.50 -5.82	13.24 -9.89
az_T [m/s^2] (Point1)	1.87 -1.24	3.75 -3.11	1.82 -1.23	2.97 -2.36	1.77 -1.26	3.02 -2.31	4.04 -3.09
ax_T [m/s^2] (Point5)	3.39 -4.04	4.99 -5.52	3.39 -4.04	3.48 -3.78	3.41 -4.05	3.44 -3.78	5.05 -5.55
ay_T [m/s^2] (Point5)	2.47 -2.62	3.63 -3.67	2.40 -2.61	2.36 -2.62	2.43 -2.70	2.35 -2.71	3.63 -3.72
az_T [m/s^2] (Point5)	0.56 -0.60	1.16 -1.21	0.54 -0.53	0.99 -1.08	0.54 -0.53	0.89 -1.08	1.18 -1.28

Table 24 Loads on the tower at the mean water level

TOWER LOADS (g.r.s.) – Point 5							
	Sim. 15	Sim. 16	Sim. 17	Sim. 18	Sim. 19	Sim. 20	Sim. 21
Mx [Nm]	393.4 -101.3	572.3 -111.5	388.6 -98.8	290.7 -40.6	389.2 -95.5	306.5 -50.8	566.7 -87.6
My [Nm]	345.6 -153.7	412.5 -271.8	345.6 -149.2	206.7 -125.1	341.2 -148.5	207.8 -129.3	412.8 -268.4

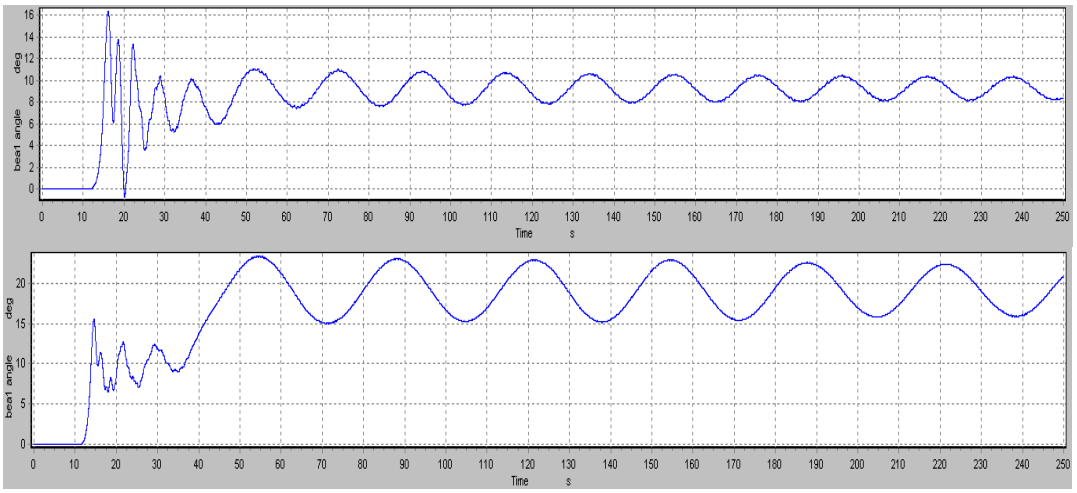

Figure 21Tilt angle time series, from top: Sim11 and Sim12

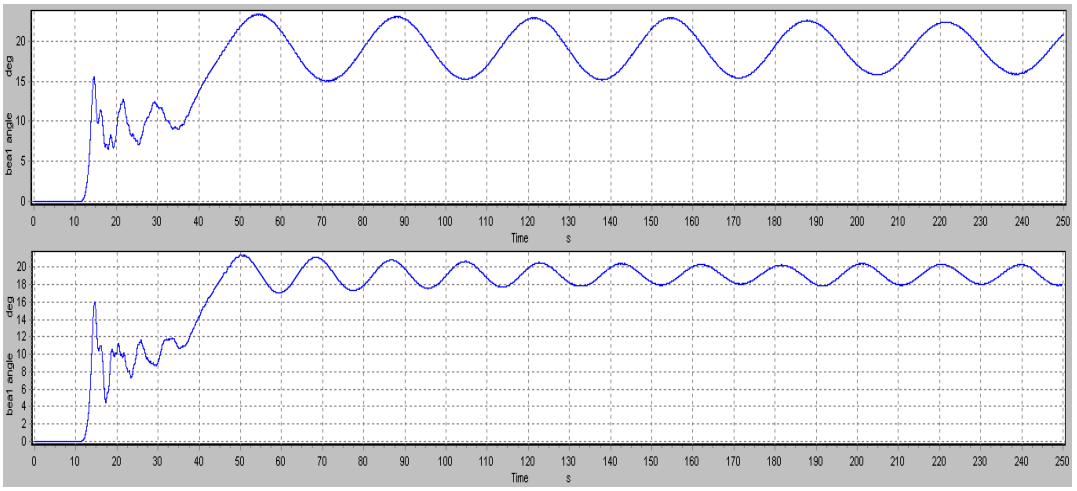

Figure 22 Tilt angle time series, from top: Sim12 and Sim12 with reduced inertia

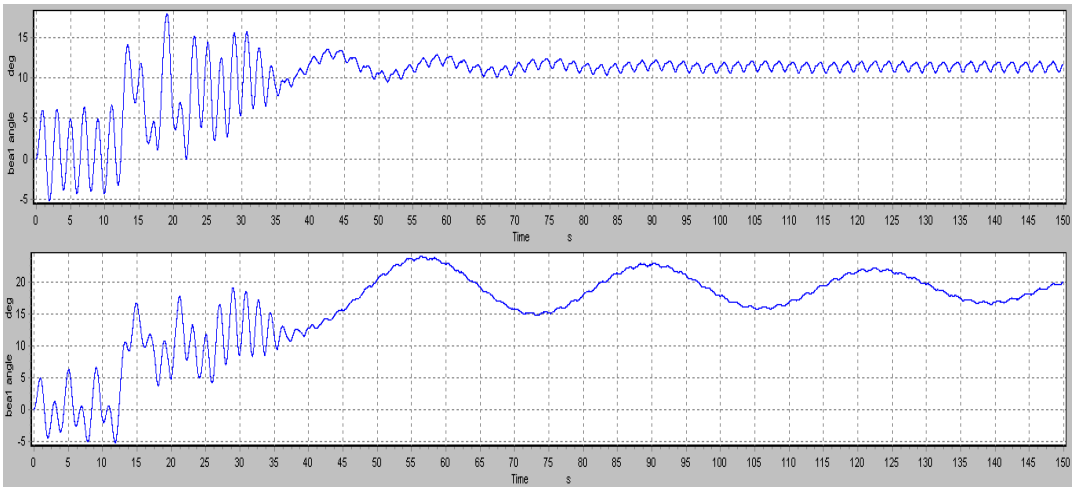

Figure 23Tilt angle time series. From top: sim17 and Sim18

At low wind speed (7m/s) and 251rpm, the most critical events seem to occur at the starting of the turbine (figure 19 top). The frequency of the wave loads is still well distinguishable (figure 21, top). At w_{sp}=12.3m/s and ω_r=440rpm, the periods of the motion in pitch increase strongly (figure 19, bottom). The contributions of the high frequency loads are less visible (figure 21, bottom). Meanwhile, the turbine has some larger oscillations, probably due to its inertia.

Among the performed simulations, the most challenging one for the equilibrium is at w_{sp}=12.3m/s and waves on the same direction of the wind (Simulation18 in table 22). The water current does not seem to give significant changes (Simulation 20, in table 22). On the other hand, the most critical loads on the tower, at the mean water level, are recorded for waves either currents perpendicular to the wind speed direction (Simulation 21 in table 24). The maximum tilt angle does not correspond to the maximum external load, probably due to the strong contribution of the inertial loads. In figure 22 the importance of the inertia at high rotational speeds is shown. The second plot in the figure is obtained by reducing the inertia of the tower.

2.6 The final DeepWind demonstrator rotor design

The second design iteration step of the demonstrator was analysed by Trento, [5]. The aerodynamic performances were analyzed taking into consideration a rotor with two or three blades with the same chord length (i.e. different solidity), of 100mm, with the NACA0018 airfoil and the DU 06-W-200 airfoil. The power and torque characteristic curves versus rotational velocity were calculated in the operating range of the demonstrator (i.e. for a wind velocity ranging from 3m/s to 16m/s). The conditions of maximum power were evaluated and the theoretical optimal power curve was traced. The loads for three different conditions were determined:

- extreme wind speed condition, i.e. 20m/s reference wind speed, with rotor in idling;
- the maximum operational wind velocity, i.e. 16m/s at the operational rotor speed;
- for an extreme condition of 10% rotor overspeed.

The final aerodynamic design of the DeepWind demonstrator rotor are shown in table 22.

One of the most important parameter to control the turbine behavior is the rotational speed. Depending on the complexity degree of the turbine, different control curves can be chosen. The aerodynamic power is limited at 1100W in order to get about 1kW of electric power. Referring to figure 27 for the two-bladed and figure 28 for the three-bladed rotors we consider three different control strategies, where the rotor speed can be:

- variable from a minimum value (point A) up to a maximum value (B) to work at the optimum aerodynamic tip speed ratio, and then fixed to limit the power (B-C), defined as Control curve 2;
- variable with the optimum tip speed ratio from a minimum value (point A) up to a maximum value (E) where the maximum power is obtained and then varied (E-C-D) to assist the stall;
- fixed speed (A'-B-C), the most simple solution from the electromechanical point of view, defined as Control curve 4.

The Control curve 2 is the most promising between the three choices, because with the variable speed it can get more power at low winds and starts at a lower cut-in wind speed (3m/s versus 6m/s of the fixed speed case. It confines the range of variability compared to the assisted stall control (though with a penalty of power at high winds) reducing the difficulty of the mechanical design to avoid resonances in the Campbell diagram. Maybe an intermediate curve between the control 2 and the control 3 could be the optimum for the real turbine.

2.6.1 Calculations of rotor torque

The aerodynamic characteristics of the blades profiles are shown in figure 24

The two- and three-bladed power and torque curves for the TUDelft DU 06-W-200 airfoils are shown in figures 25 and 26. The power is additionally shown in figures 27 and 28. Compared to calculations of NACA0018 airfoils [5] there is a reduction of the maximum rotor speed, partly due to the better performances of the DU airfoil, partly to the little camber added to the airfoil compared to NACA0018 and partly to the higher deep stall angle and post stall characteristics. This is absolutely beneficial from the mechanical point of view due to lower centrifugal forces and rotor imbalance effects. The performances are about 4% better at the design wind speed of 7m/s. The difference gets a little higher for stronger winds. At cut-in speed the rotor speed is lower too, and the starting characteristics should be slightly improved. On the other hand the maximum power is attained at about 15m/s compared to the 14m/s of NACA0018 and the torque demanded to the generator is higher due to the slower rotational speed. Globally the DU 06-W-200 is better performing compared to NACA0018.

Table 22 – Troposkien configuration and geometrical characteristics of the DU 06-W-200 Darrieus wind turbines analyzed.

Height	2.00 m
Diameter	2.00 m
Swept area	2.55 m^2
Rotor aspect ratio	1.0
Blade length	2.93 m
Blade chord	0.10 m
Blade profile	DU 06-W-200
Blade geometry	Troposkien
Number of blades	2 3
Solidity [=Bc/R]	0.2 0.3

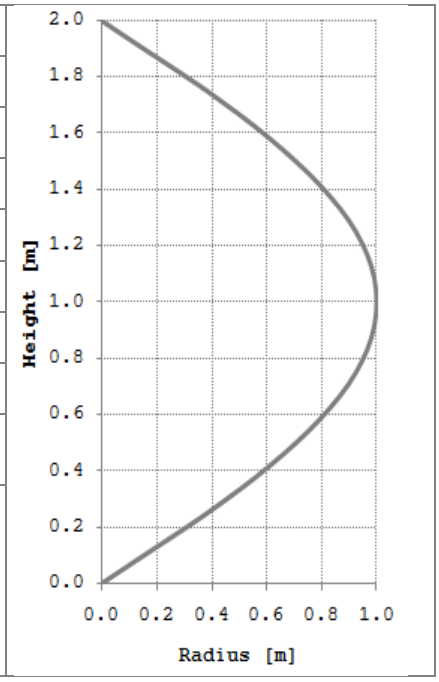

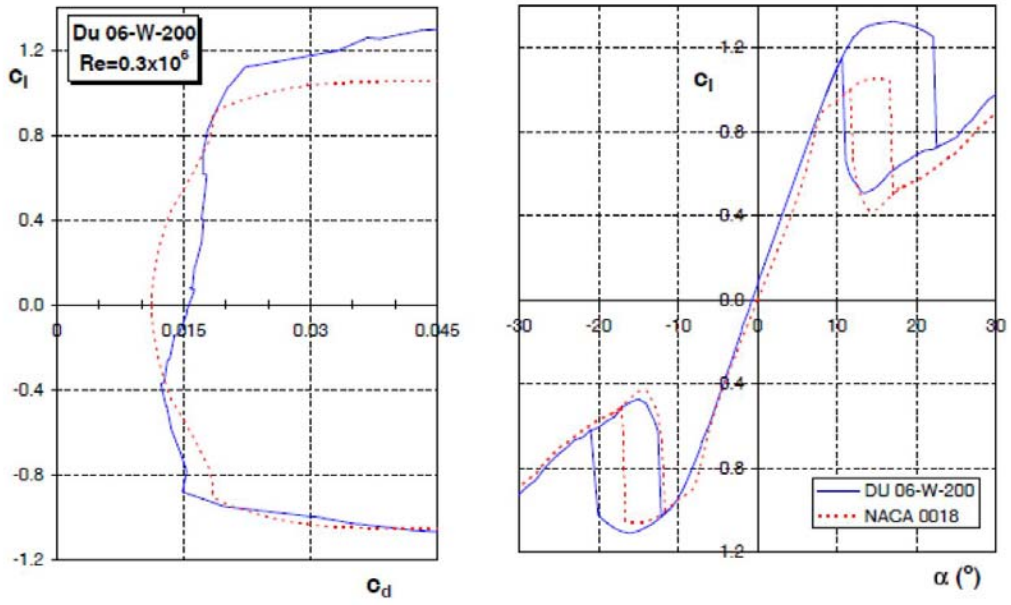

Fig. 24 Drag polars and lift curves of DU 06-W-200 and NACA 0018 profiles provided by TUDelft

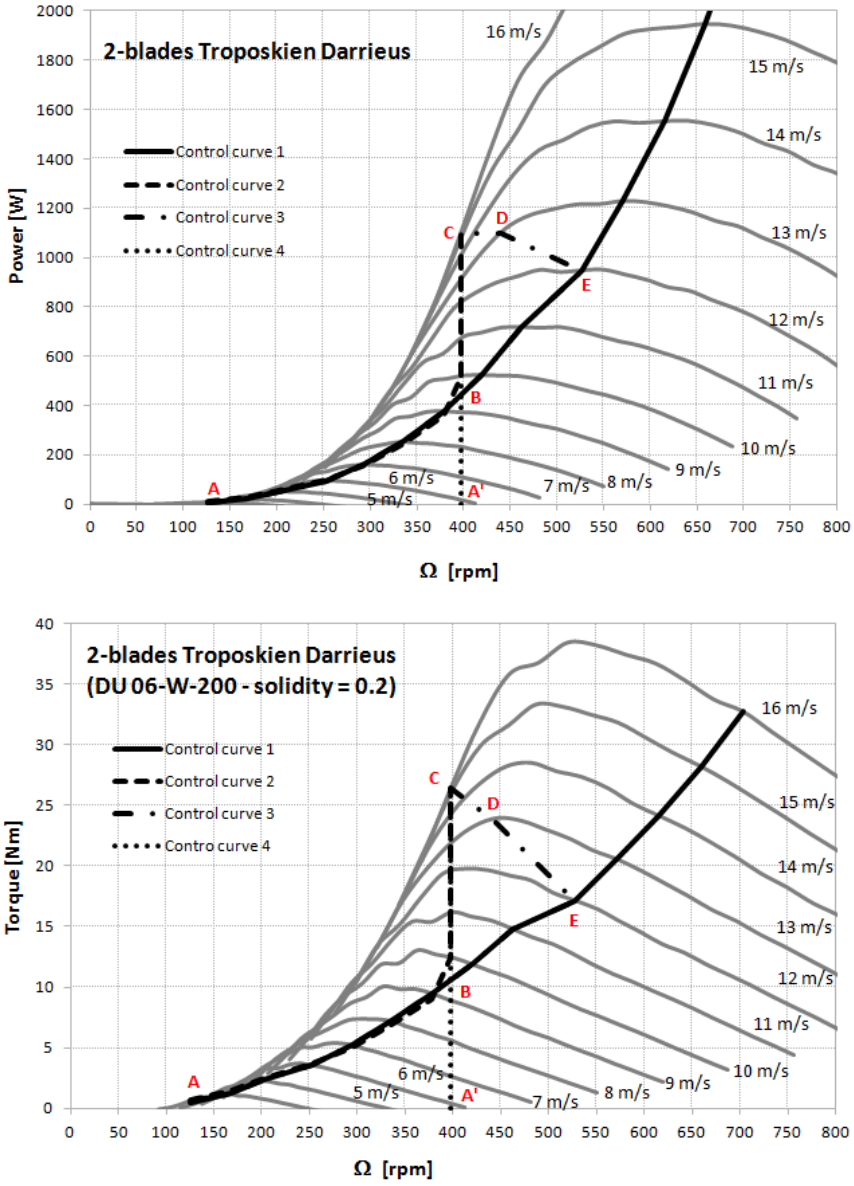

Fig. 25 - Comparison between the aerodynamic power (above) and torque (below) versus rotor rotational speed for the DU 06-W-200 2-bladed Darrieus turbine.

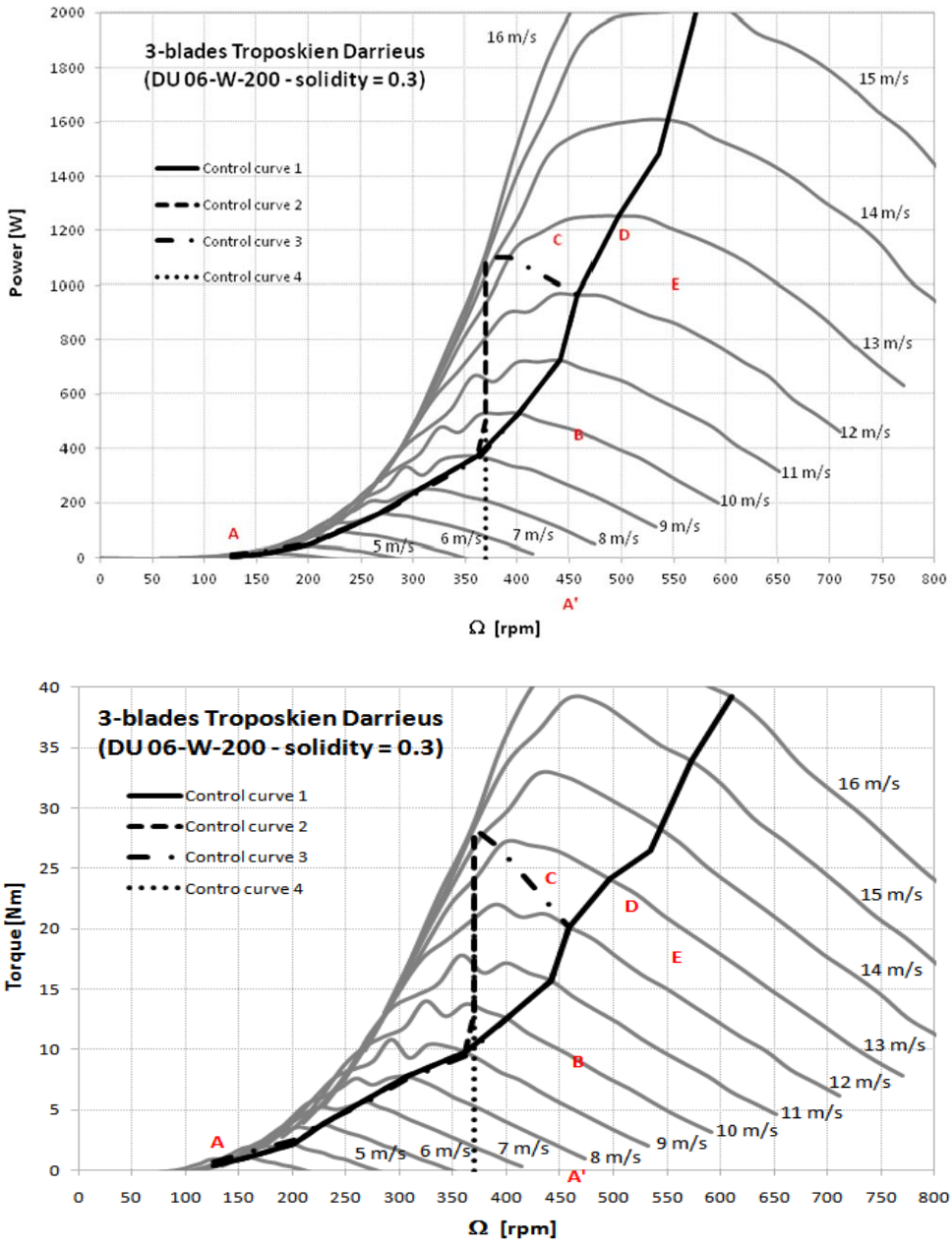

Fig. 26 - Comparison between the aerodynamic power (above) and torque (below) versus rotor rotational speed for the DU 06-W-200 3-bladed Darrieus turbine.

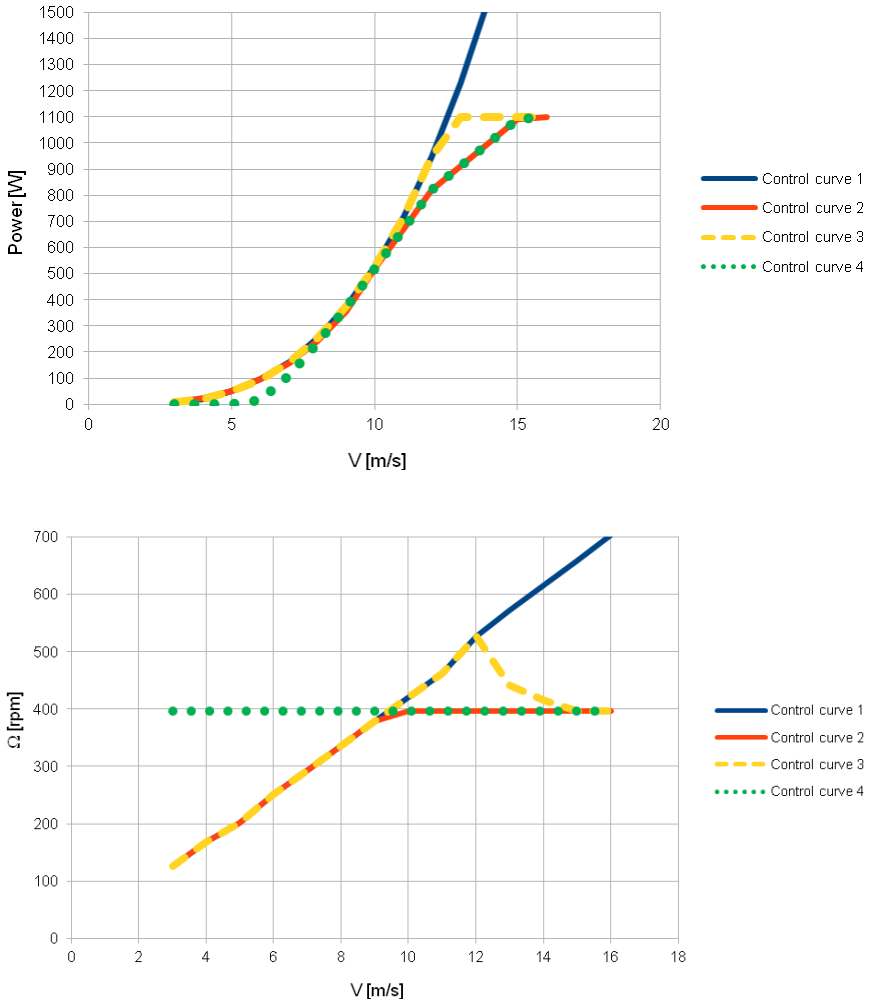

Fig 27 - Comparison between the aerodynamic power (above) and rotational speed (below) versus wind speed for the DU 06-W-2002-bladed Darrieus turbine.

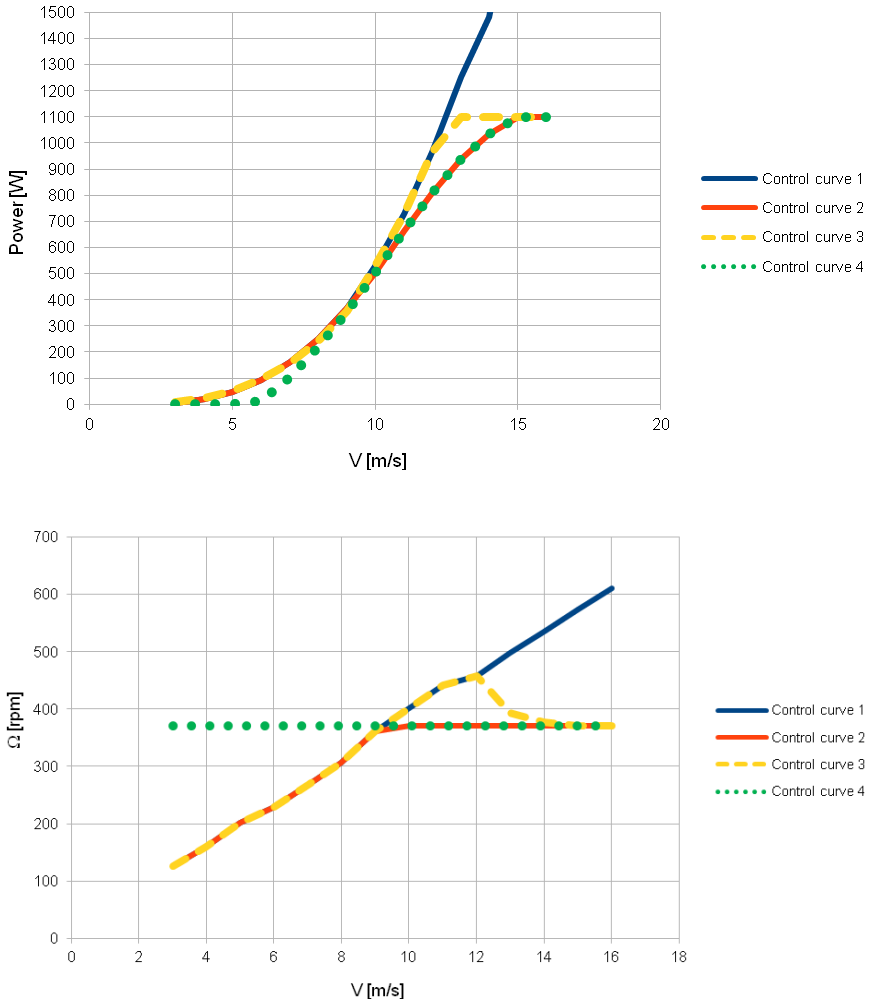

Fig 28 - Comparison between the aerodynamic power (above) and rotational speed (below) versus wind speed for the DU 06-W-200 3-bladed Darrieus turbine.

2.6.2 Calculations of extreme loads at 0 rpm and 20 m/s

The extreme loads at stopped condition and 20m/s were calculated, see figure 29 for the two bladed rotor and figure 30 for the three bladed rotor. The average thrust in streamwise direction is reduced both for two and three-bladed rotor of about 5%, while in the transverse direction it is almost null with the TUDelft profile. The only case where there is an increase of the load is for the minimum side force for the three-bladed turbine, but this is not relevant.

Table 25 – Comparison of the different operational loads in idling condition at V0 = 20 m/s (DU 06-W-200 Darrieus turbine).

	2-bladed DU 06-W-200	3-bladed DU 06-W-200
Rotor rotational speed [rpm]	0	0
$Fx_{,AVE}$ [N]	69.81	102.26
$Fx_{,MAX}$ [N]	153.22	112.39
$Fx_{,MIN}$ [N]	1.85	87.08
$Fy_{,AVE}$ [N]	-3.79	-5.72
$Fy_{,MAX}$ [N]	55.03	25.76
$Fy_{,MIN}$ [N]	-65.83	-37.42
$T_{,AVE}$ [Nm]	-0.55	-0.80
$T_{,MAX}$ [Nm]	5.97	4.46
$T_{,MIN}$ [Nm]	-2.65	-2.95

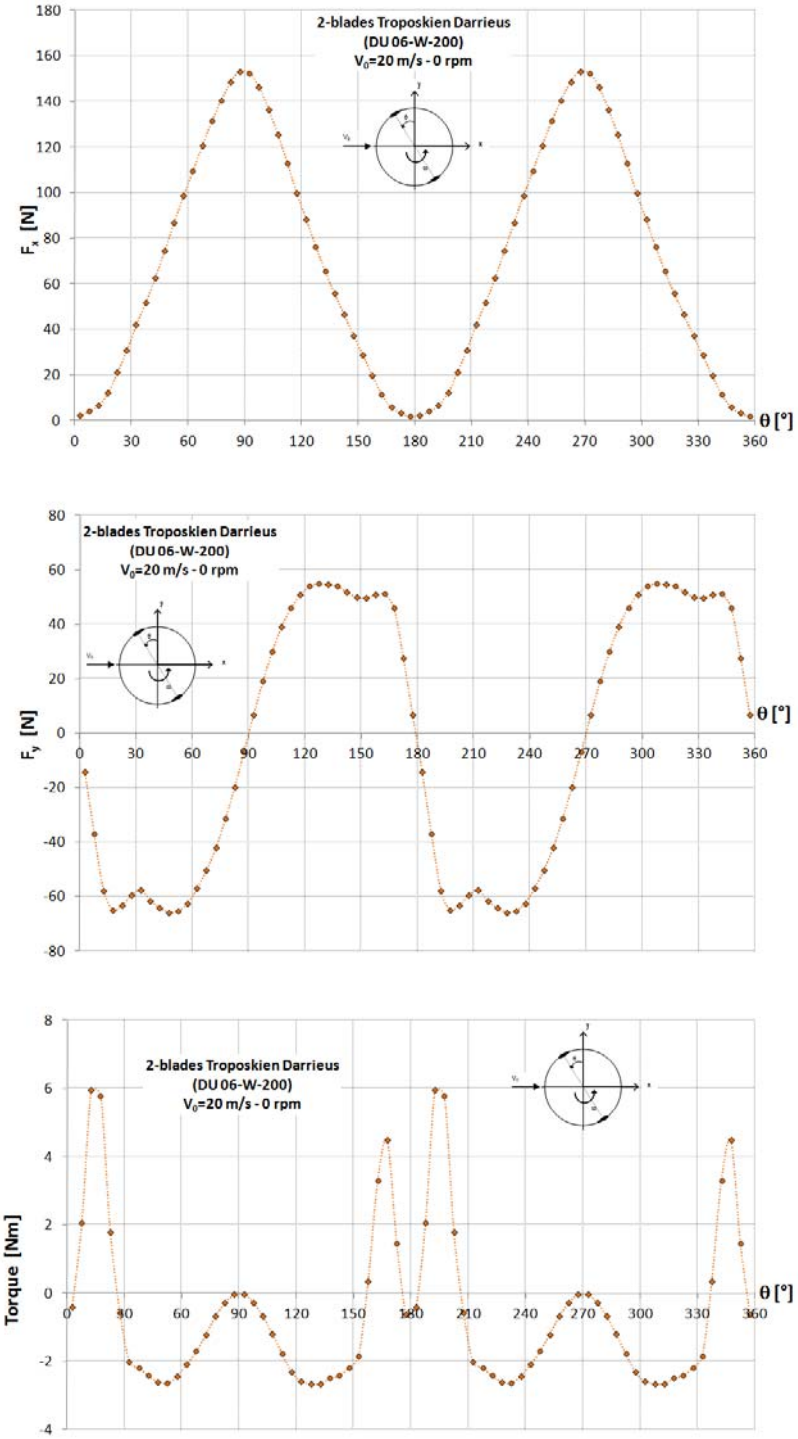

Fig. 29 - Comparison between the streamwise thrust (above) and transverse one (below) versus azimuthal position for the DU 06-W-200 2-bladed Darrieus turbine.

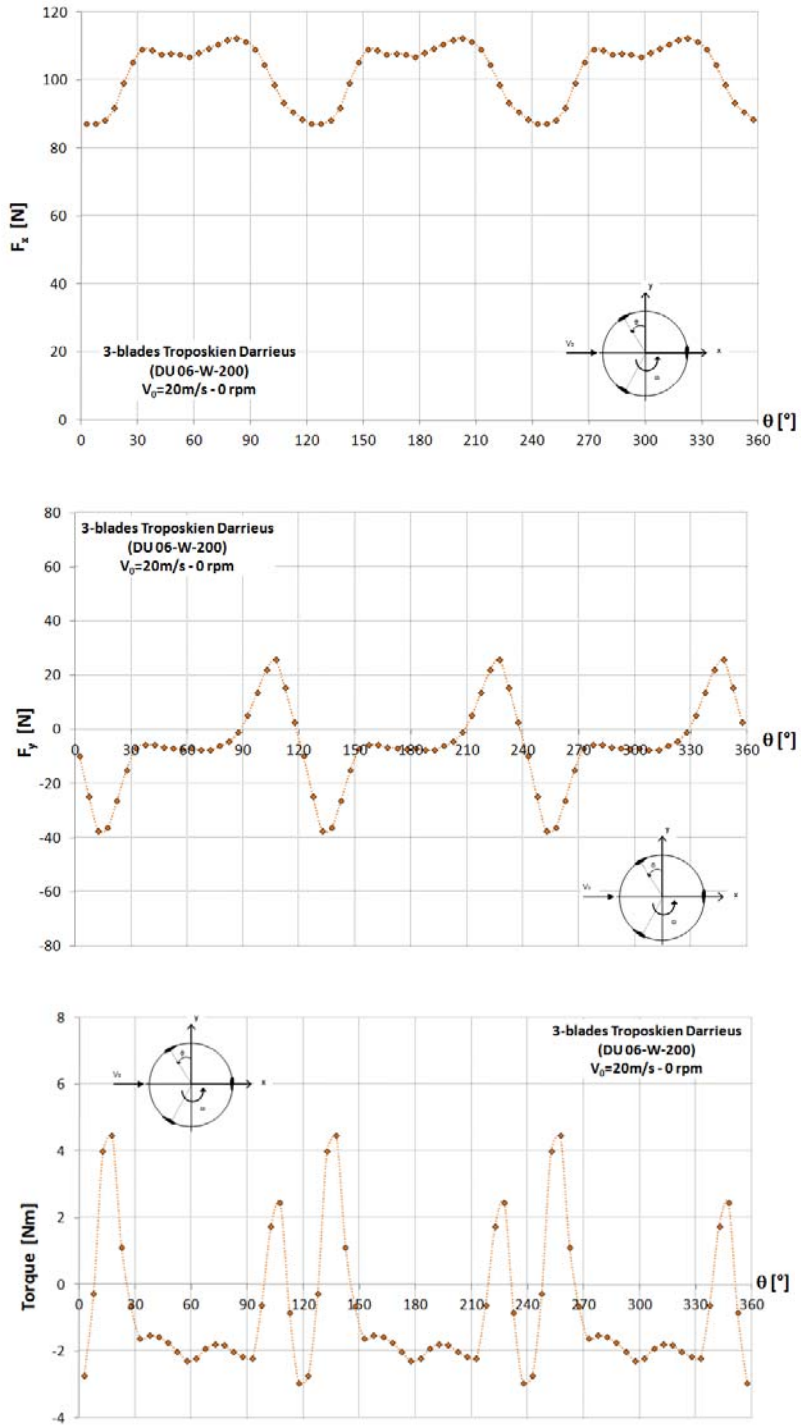

Fig 30 - Comparison between the streamwise thrust (above) and transverse one (below) versus azimuthal position for the DU 06-W-200 3-bladed Darrieus turbine.

2.6.3 Calculations of operational loads at 397 rpm (2-blades) and 370 rpm (3-blades) and 16 m/s

The general behavior of the forces with the DU 06-W-200 airfoil is similar to the case with NACA0018 airfoil, see figure 31 and 32.

The maximum operational streamwise averaged forces with the new airfoil are reduced of about 5-6% for both configurations. There is an important increase of the mean side forces which are approximately doubled. The ranges of the forces are slightly lowered for the two-bladed configuration, while for the three-bladed there is a small increase. There is a neat increase of the mean torque with an unchanged torque range for the two-bladed rotor.

Table 26 – Comparison of the different maximum operational loads at V0 = 16 m/s.

	2-bladed DU 06-W-200	**3-bladed DU 06-W-200**
Rotor rotational speed [rpm]	**397**	**370**
$Fx_{,AVE}$ [N]	147.09	185.92
$Fx_{,MAX}$ [N]	287.17	256.53
$Fx_{,MIN}$ [N]	3.74	103.89
$Fy_{,AVE}$ [N]	-35.03	-50.86
$Fy_{,MAX}$ [N]	154.23	44.81
$Fy_{,MIN}$ [N]	-238.10	-134.56
$T_{,AVE}$ [Nm]	26.40	29.94
$T_{,MAX}$ [Nm]	56.55	64.26
$T_{,MIN}$ [Nm]	-3.71	-14.56

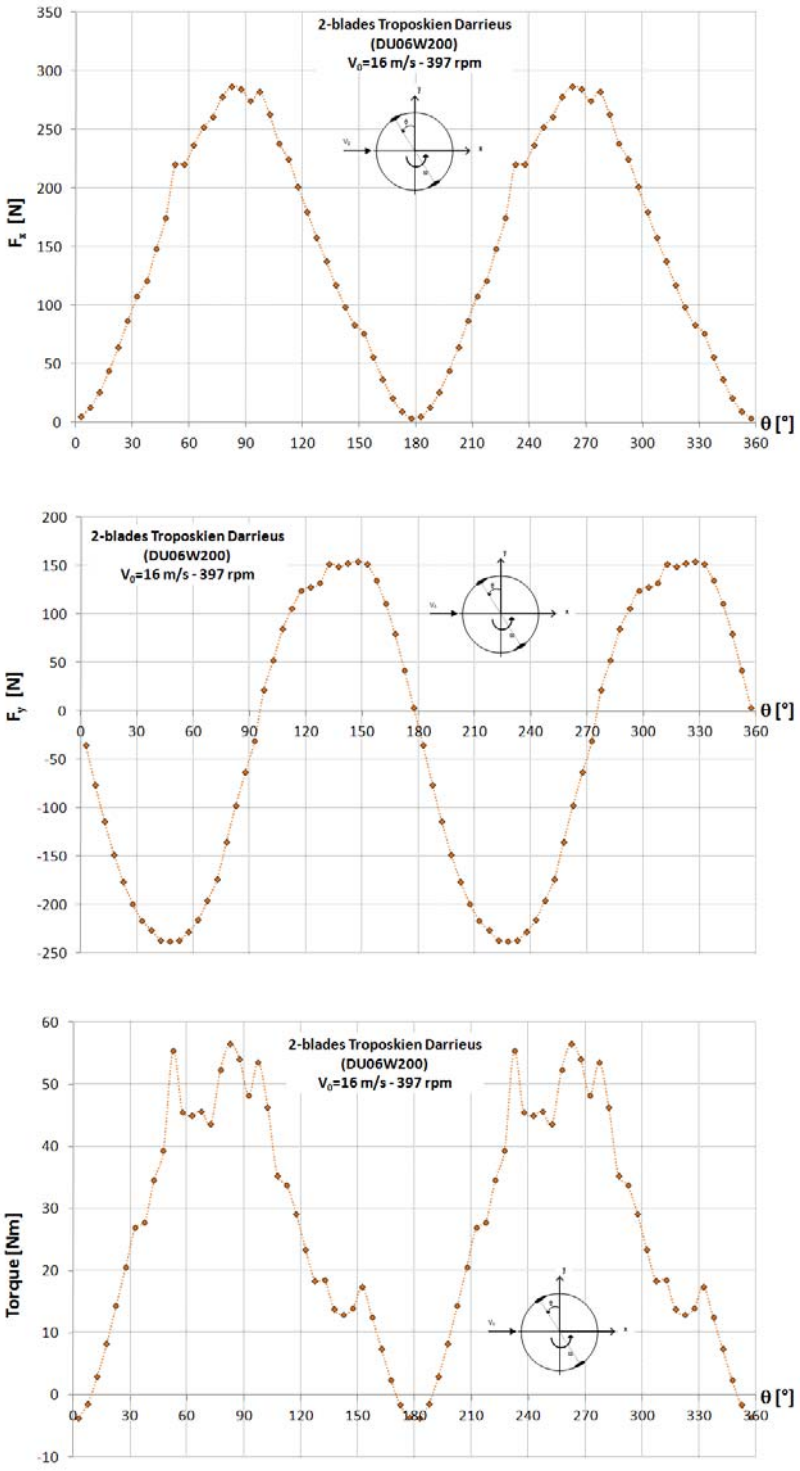

Fig. 31 - Comparison between the streamwise thrust (above) and transverse one (below) versus azimuthal position for the DU 06-W-200 2-bladed Darrieus turbine.

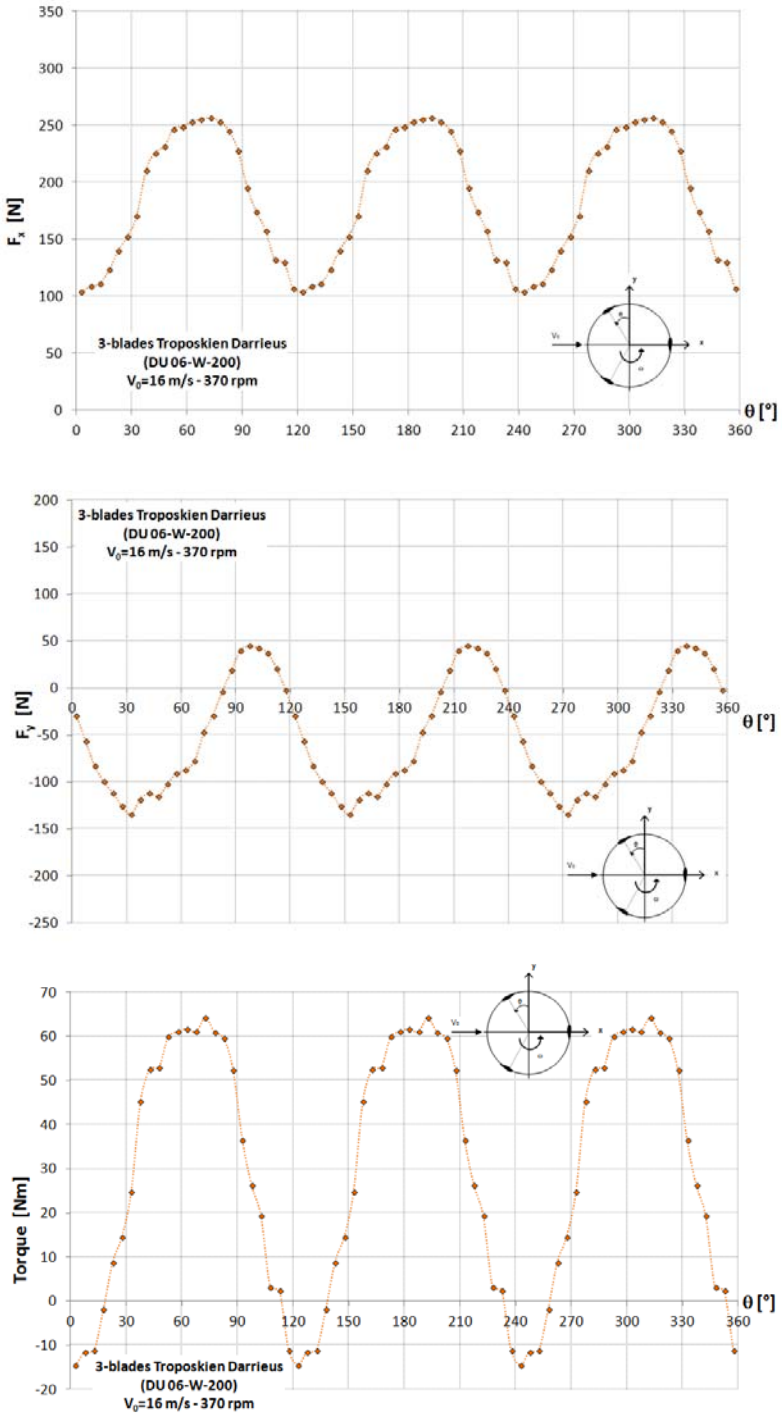

Fig. 32 - Comparison between the streamwise thrust (above) and transverse one (below) versus azimuthal position for the DU 06-W-200 3-bladed Darrieus turbine.

In the report [5] the final rotor geometry has been analyzed with four different configurations, two and three-bladed rotors with NACA0018 and TUDelft DU 06-W-200.

The aerodynamic torque and power curves have been calculated in order to evaluate different control strategies. This is a fixed pitch turbine so to control the aerodynamic power at the shaft the considered possibilities have been stall regulation, skewing the rotor from the wind, acting on the airfoil characteristics (boundary layer control, active trailing edges, etc.) or a mix of them. We chose the first way for its simplicity.

The variable speed with passive stall regulation has been taken as the reference control strategy, and compared with the fixed speed regulation and the assisted stall regulation.
For the demonstrator the reference control is the best compromise between the three choices, because with the variable speed it can get more power at low winds and starts at a lower cut-in wind speed (3m/s versus 6m/s of the fixed speed case), and it confines the range of variability compared to the assisted stall control (though with a penalty of power at high winds) reducing the difficulty of the mechanical design to avoid resonances in the Campbell diagram.

Comparing the two different airfoils emerges that with DU 06-W-200 there is a reduction of the maximum rotor speed, partly due to the better performances of the airfoil, partly to the little camber added to the airfoil compared to NACA0018 and partly to the higher deep stall angle and post stall characteristics. This proves beneficial from the mechanical point of view due to lower centrifugal forces and rotor imbalance effects. The starting characteristics are slightly improved. The maximum power is attained at about 15m/s for TUDelft airfoil compared to the 14m/s of NACA0018 and the torque demanded to the generator is higher due to the slower rotational speed. Globally the DU 06-W-200 is better performing compared to NACA0018.

The design extreme wind speed averaged over 10 minutes has been set to 20m/s. The 3 seconds averaged wind speed can be estimated about 28m/s. The average torque is negative for all the configurations, so the rotor should not self-start in static conditions, but dynamically the behavior could be different. The TUDelft airfoil gives values near zero, the self-starting capability is plausible.

The torque and forces fluctuations for the two-bladed rotor are very high over the 360°. The azimuthal position of stable equilibrium is about ±15-25°, both for two and three bladed rotor. In this position the streamwise force is at minimum and the side force at maximum. So in a conservative way the design forces could be taken as the average value for the streamwise force and the maximum value for the transverse force. The average thrust in streamwise direction is reduced both for two and three-bladed rotor of about 5% with the DU 06-W-200 profile.

The maximum loads at the cut-out velocity of 16m/s could be a reference for the range of loads in normal conditions. Comparing the forces for the two rotors we see that both in streamwise and transverse direction the three-bladed rotor has higher average values (important for the stability of the buoy) but lower ranges of fluctuations.

The fluctuations range of the aerodynamic torque is between two and three times the mean value. In the range of the variable rotational speed this should not be a problem for the generator, due to the high polar inertia of the system, but more care should be put on the control stiffness at fixed speed, limiting the maximum torque applied with the generator and contemporaneously the rotor speed fluctuations.

We took as an extreme operational condition an overspeeding of 10% at the cut-out wind speed of 16m/s due to rotor speed fluctuations or generator loss and intervention of the safety brake (electrical or mechanical). The case of overspeeding at cut-out wind speed with the case of extreme wind of 28m/s are the most stressing for the structure and the stability of the system.
The difference on the average forces are quite important, with a raise of about 20% or even more for three-bladed rotor. With the TUDelft airfol the streamwise mean forces are reduced of 6-7% while there is an important increase of the mean side forces which are approximately doubled. The mean torque overshooting is lower than 30% compared to about the 40% with the NACA0018. The generator and the brake should be accordingly dimensioned.

A last consideration must be done on the airfoils database extension for post-stall data. This issue has proven crucial for the peak power prediction and forces evaluation up to the cut-out wind speed, and intimately conjugate with the dynamic stall phenomenon in VAWT. The procedure for extending the database has been improved, but a general investigation should be done to reduce the uncertainties of VAWT in stalled conditions.

3. Manufacture of the DeepWind demonstrator

The DeepWind demonstrator was manufactured by the different partners of work package 7. Vestas manufactured the foundation, torque arm, gimbal joint and turbine rotor. Aalborg University manufactured the generator box, the control system and provided cabling from test site to land. DTU provided the instrumentation and data transmission system in the rotor, the concrete feet, the mast, mast instrumentation, data transmission to land, the ADCP, and the sea vessel for installation and maintenance. Nanuphar manufactured the blades.

3.1 Blades

The GRP blades were designed by DTU and Nanuphar. The blade profile was the DU- 06-W-200 profile, see figure 33. This profile is used both for the 2 and 3 bladed rotors.

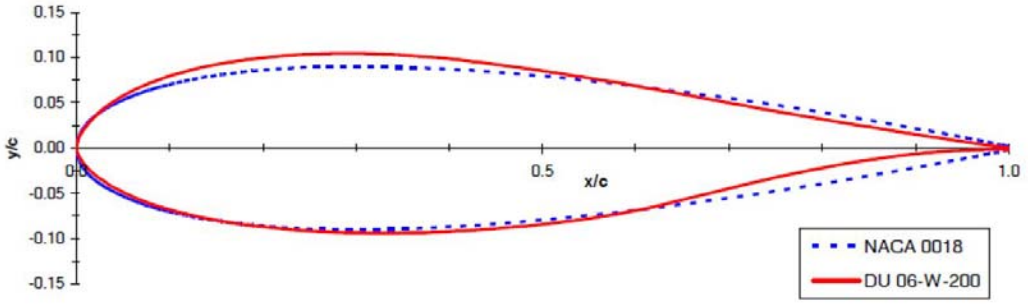

Fig 33 Graph of the DU 06-W-200 profile compared to the NACA 0018 profile provided by TUDelft

The structural properties are based on the loads calculated for the 2 bladed rotor. The blade has the same outer geometry trough the length of the blade but the structural properties change along the blade. The structural properties do not change gradual along the blade, but only at the intersection between the different sections of the blade, see tables 27 to 29.

Table 27 Internal structural properties of the blade root section from blade root to 620mm from the blade root

HAWCK2 input data – Blade root - 2 bladed rotor		
Parameter	Value	Units
m	0.883	kg/m
A	4.22E-04	m^2
I_1	1.69E-09	m^4
I_2	3.09E-08	m^4
E	1.60E+10	N/m^2

Table 28 Internal structural properties of the middle section from 620mm to 1060mm from the blade root

HAWCK2 input data – Middle section - 2 bladed rotor		
Parameter	Value	Units
m	0.674	kg/m
A	3.27E-04	m^2
I_1	1.34E-09	m^4
I_2	2.36E-08	m^4
E	1.60E+10	N/m^2

Table 29 Internal structural properties of the tip section from 1060mm form the blade root and across the symmetrical axis

HAWCK2 input data – Tip section - 2 bladed rotor		
Parameter	Value	Units
m	0.410	kg/m
A	1.97E-04	m^2
I_1	8.44E-10	m^4
I_2	1.44E-08	m^4
E	1.60E+10	N/m^2

The blades for the demonstrator were manufactured by Nanuphar. The blades were made in glassfiber reinforced composite with a shell and bar structure as seen in figure 34.

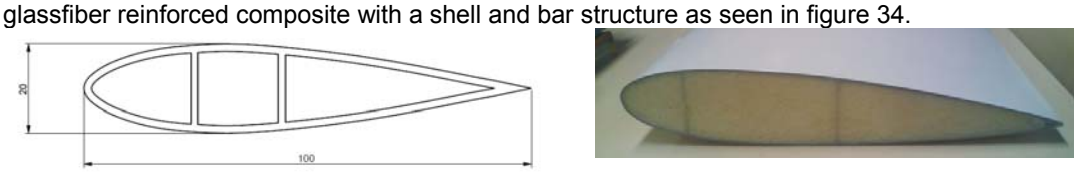

Fig 34 Profile structure of blades from Nanuphar (this profile is made for a larger blade)

The blades were produced in a mould, where glass-fibre was laid up over the foam cores and epoxy was then injected into the closed mould, see figure 35. The blades were then cured very slowly. The mounting of the blades to the shaft was not part of the Nanuphar blades. DTU designed fittings to glue on the blades. These are shown in figure 36.

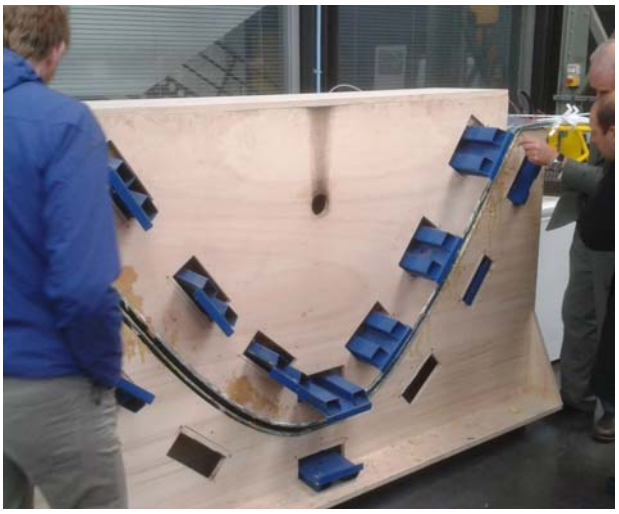

Fig. 35 Picture of mould for production of the GRP blades by Nanuphar

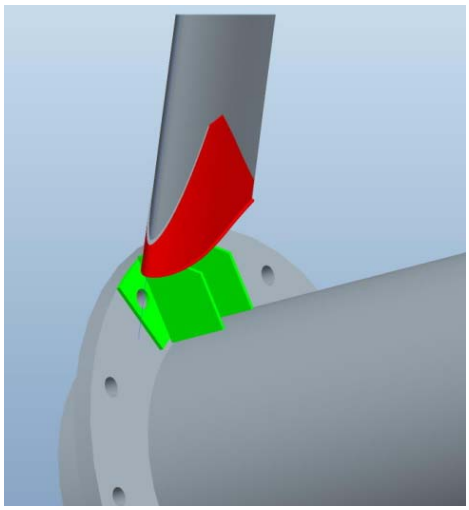

Figure 36 Fittings made by DTU for mounting the Nanuphar blades on the rotor.

The first set of three blades delivered by Nanuphar was inspected for profile geometry [10]. The inspection showed, unfortunately, some severe defects, both of the profile shape and of the surface smoothness. A template of the specified profile was produced and the blades profiles were compared to the template. The defects were found to be the same on all three blades, see figure 37. The defects also showed to be general over the entire length of the blades.

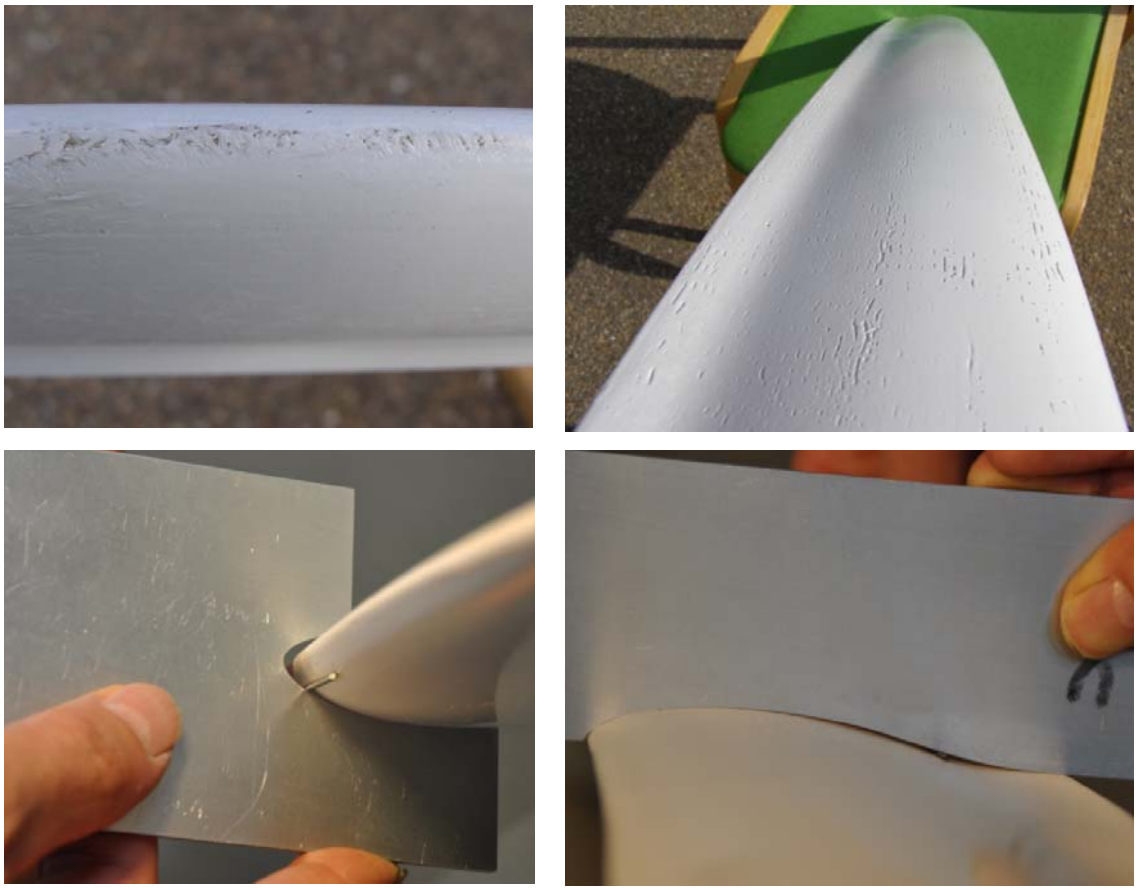

Figure 37 Inspection results of the first set of blades from Nanuphar for the DeepWind demonstrator. Upper left, surface defects at the leading edge. Upper right, surface defects on the pressure side. Lower left, profile deviation from specified template profile at leading edge. Lower right, profile deviation from specified profile at pressure side.

On the basis of the defects it was found necessary to look at alternative providers of blades. A manufacturer of small vertical axis wind turbines, Windpower Tree, were able to deliver three blades in circular shape. These blades were made in extruded aluminium and bent in circular shape. The profiles have a chord of 120mm and a SAND0018/50 profile [11]. This profile is tailored for vertical axis turbines and is expected to be a better than the NACA0018 profile. It was decided to initiate tests with these blades, and a set of three blades were ordered. Two such blades from Windpower Tree are seen on the rotor tube in figure 38.

Figure 38 Windpower Tree blades mounted on the demonstrator rotor tube.

Another set of three improved blades were produced by Nanuphar. These blades did not have the surface defects, but were smooth. The deviations in the profile, however, was the same. Nanuphar measured the profiles in a measurement bench, and delivered a report on the coordinates.

In Roskilde fjord only the configuration with two Windpower Tree blades was tested. At Marin basin both the configuration with two Windpower Tree blades and the one with three Nanuphar blades were tested.

3.2 Rotor tube

The rotor tube was manufactured by Vestas. The drawings are shown in figure 39. The total length of the rotor is 5.00m, outer diameter 0.15m and wall thickness 5mm. The tube is made of standard extruded aluminium AW 6082 T6, and the flanges for blade attachment are welded on. The rotor flanges were made to take two or three blades. The rotor tube was supplemented with more buoyancy, see figure 40, due to a heavier rotor than expected (tube wall thickness was not available in 3mm but only in 5mm). The outer diameter of the buoyancy part is 400mm.

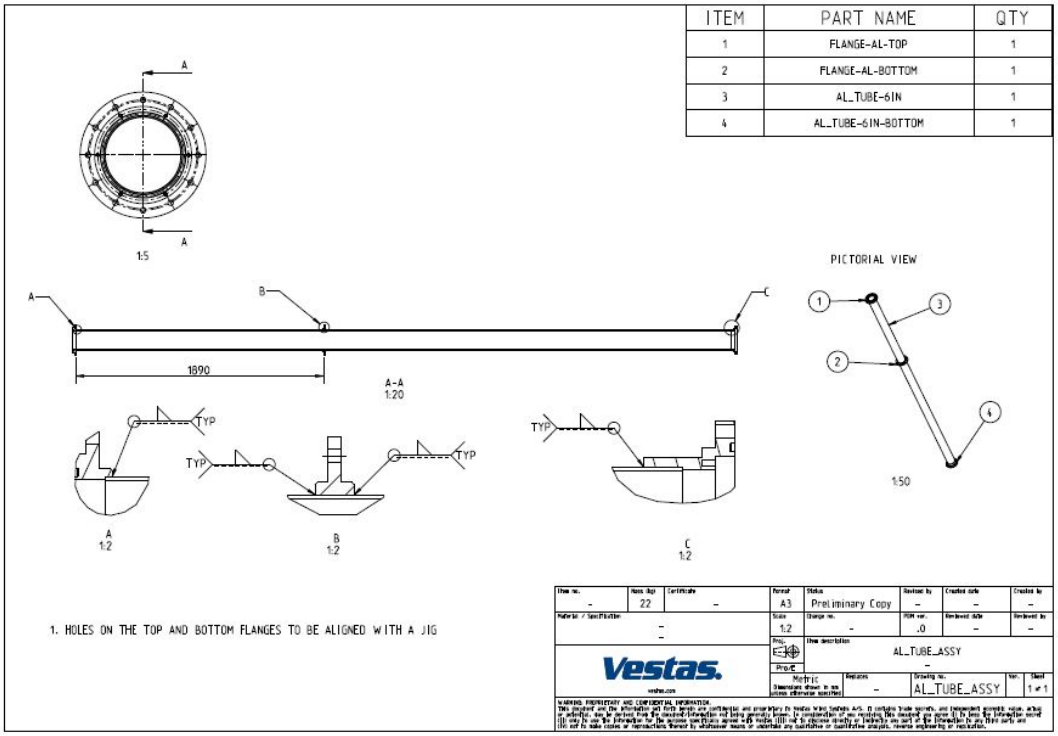

Figure 39 Rotor tube manufactured by Vestas

Figure 40 Rotor tube with buoyancy lying on the ground

3.3 Generator box and control system

The generator box was designed and manufactured by Aalborg University. The cylindrical box was made in stainless steel. The generator was a Leroy Somer 1.1kW asynchronous motor with a fail-safe disc brake that needs a voltage signal to detach before operation can start. A belt drive with a gearing ratio of 1:3.41 is used to increase wind turbine rotor speed from nominal 400rpm to nominal 1500rpm of generator. In the generator box a slip ring was mounted on the external shaft to provide power for the instrumentation in the rotor tube. The generator box is seen mounted in the gimbals joint in figure 41.

3.4 Foundation setup

The foundation was designed by Vestas. The requirements to the foundation was that it was heavy enough to stand stable on the sea bed but also light enough to transport to site and to get off the sea bed again. Figure 41 shows a drawings of the foundation setup with the mast and generator box in place. The assembly of the foundation with concrete feet, generator box and torque arm with air barrels for lifting and level control are shown in figure 42.

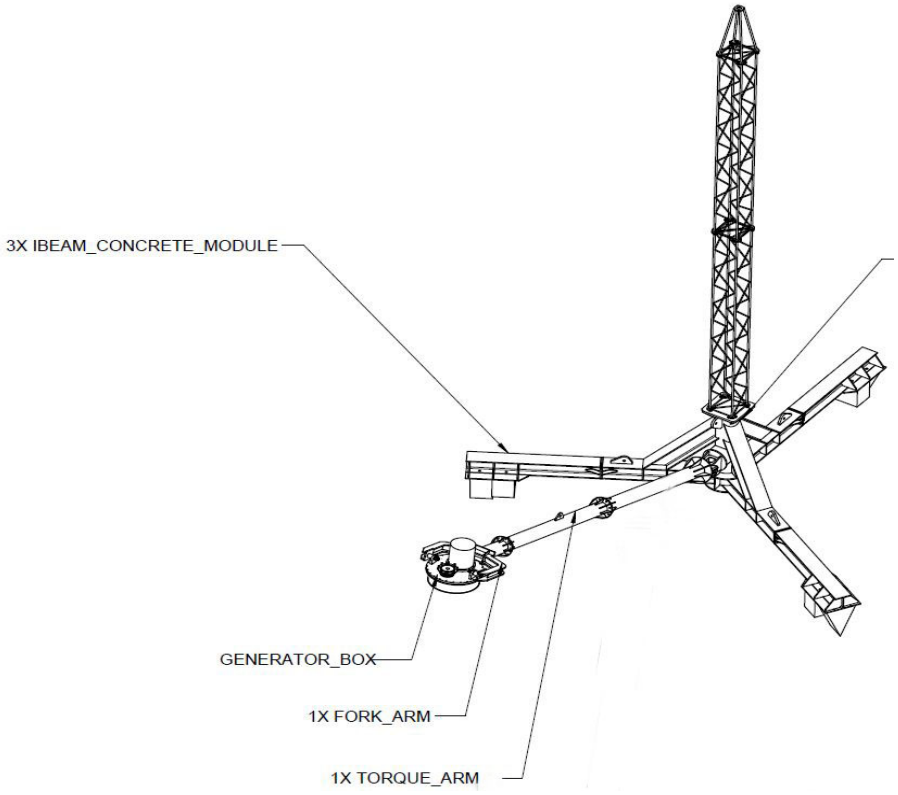

Figure 41 The foundation setup with the three legs, the mast, the torque arm, and the generator box on the gimbals joint.

Figure 42 The foundation with concrete feet standing on the pier. On the torque arm the generator box and the air barrels are mounted.

4. Instrumentation

The instrumentation of the rotor was based on the objectives of measurement of movements of the rotor. For this reason and to keep the weight low no load measurements were made on the rotor or the rotor blades. The instrumentation in the rotor consisted in the bottom of a National Instruments measurement system, powered by a power supply through the generator box. A 3D accelerometer and a gyroscope was also mounted in the bottom. Additionally a 3D accelerometer was mounted in the rotor top. Data were transmitted wirelessly from the top of the rotor to the mast. The mast was instrumented with a 3D sonic, and a temperature and pressure sensor. Rotor and mast data were connected at the mast and transmitted wirelessly to land. A Sentinel ADCP was installed at sea bed on the site to measure sea currents and wave heights. The ADCP was connected via cable to the measurement system in a container at the pier. A video camera was installed above the container on the pier in order to visually record the behaviour of the turbine.

The specifications of the instrumentation are shown in tables 30 and 31. The instrumentation in the rotor tube and the ADCP are shown in figure 43.

Table 30 Rotor sensors and data acquisition system

HARDWARE		
cDAQ		
	NI CompactDAQ 1-Slot Wi-Fi Chassis	1
POWER SUPPLY		
	smart guard	1
	charger	14
	LiPo battery 14.8 V 40/3C	28
STRUCTURAL SENSORS		
	Accellerometer 3 axis Seika SB3Gi	2
	cables	2
	inclinometer, seika (forseglet)	1
	cables	1
	Bricett INN-107 - 3.2 gyroscope	1
DATA TRANSMISSION SYSTEM		
	antenna + cables	1
	pc ashore	1

Table 31 Mast sensors and data acquisition system

HARDWARE		
DATA Acquisition		
	P2858a DAU	1
	Signal mast cabel	1
	Supply mast cable	
ENCLOSURE		
	P3125A DAU/Transmitter enclosure	1
TRANSMISSION		
	moxa	1
	cisco	2
	cables	1
MAST SENSORS		
	Humidity & Temp. Probe Vaisala HMP 155	1
	Radiation Shield	1
	Cable termination	1
	Cable 1x10m	1
	Metek sonic - not heated	1
	Cable for sonic 10m	2
	Barometer PTB110A	1
	Bomme incl. bardunering	1
NAVIGATIONAL AIDS		
	Aviation lights, mounted 2 m below mast top. 2 LED85AR	0
	Marine lights, mounted on platform: 2 FA249LED	1
SEA		
	ADCP:Workhorse Sentinel 1200kHz	1
	Directional Wave Array $ 3.605	1
	External battery case? $ 2.987	0
	100 m armed cabel & tripod	1

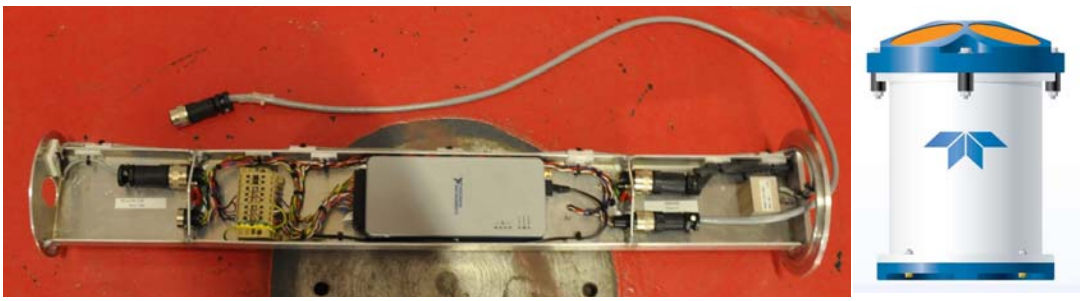

Figure 43 The rotor instrumentation, left, and the ADCP, right

5. Structural dynamics

Modal testing has been carried out by Vita on the demonstrator and a comparison has been made to a finite element model analysis with the ANSYS code of the wind turbine by Kragh [12]. The purpose was to provide a good documentation of the demonstrator structural dynamics in terms of safety and controls.

5.1 Model

The finite element model is produced in accordance with the drawing of the rotor, see figure 39. The flanges are modelled as solid bodies consisting of both the actual flanges and the part of the pipes that is connected into the flanges. The pipes and blades are modelled using shell elements. Three models are designed; see figure 44, that shows the three models: tube alone, tube and blades, and tube and blades mounted on a rigid structure that is free to rotate around one axis.

Figure 44 The three implemented FE models, tube alone, tube with two blades, tube with blades and generator box

The two first configurations correspond to the configurations that have been tested experimentally with the B&K PULSE Modal test and analysis package, see figure 45. The modal testing was conducted by hammering at a fixed point of the rotor top and simultaneously measuring the accelerations at different positions on the structure. With the method the systems transfer function is found and allowing to derive the modal shapes.

The last configuration is similar to the operating configuration; see figure 46, but neglecting the hydrodynamics, and the torsional stiffness of the support tube. The hinged support of the third model is modelled to have the same mass and centre of mass as the hinged support of the experimental demonstrator. The two clamped models are used to tune the FEM model to match the experimental results.

Figure 45: Setup of the experimental modal analysis of the tube alone (left) and the tube with blades (right).

Figure 46: Rotatable support in gimbals joint of demonstrator generator on which the rotor is mounted on the right

5.2 Support uncertainty

As seen from figure 47 right, the structure is in the experiment clamped to an aluminium plate that is mounted on a crane structure. The stiffness of this support structure is unknown. The support is modelled as an aluminium plate that is clamped at the four edges, see figure 47 left. The stiffness of the plate is tuned such that the first Eigen frequency of the tube alone model matches the first Eigen frequency that was found from the corresponding experimental results.

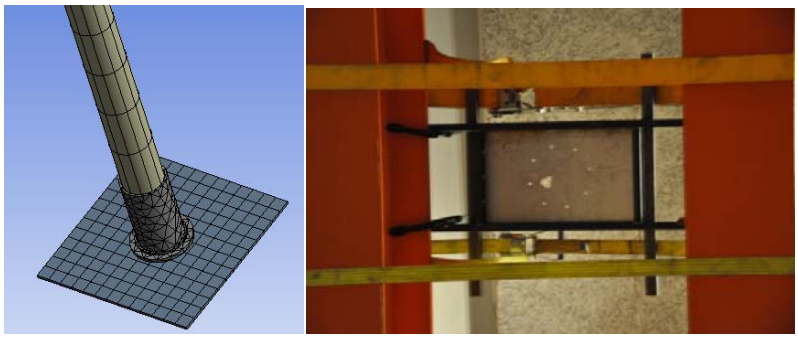

Figure 47: Modelling of the support (left) and the actual support (right)

5.3 Results

Results from 3 computations are presented: tube alone (clamped), tube and blades (clamped), and tube and blades mounted on a hinged support. The results of the two clamped models are compared to the experimental modal analysis results. For the third configuration no experimental validation is available.

5.4 Tube alone

Since the structure is symmetric, each Eigen frequency represents two orthogonal mode shapes. The stiffness of the support plate has been tuned such that the first FE Eigen frequency matches the first experimental Eigen frequency. From table 32 it is seen that there is a good match at all frequencies. The FE mode shapes are shown in figure 48.

Table 32: FE Eigen frequencies and experimental Eigen frequencies and mode shapes

FEM	**Experiment**	
Eigen fr.	Eigen fr.	Mode shape
2.78 Hz	2.75 Hz	First bending
23.61 Hz	21.75 Hz	Second bending
69.4 Hz	68.25 Hz	Third bending

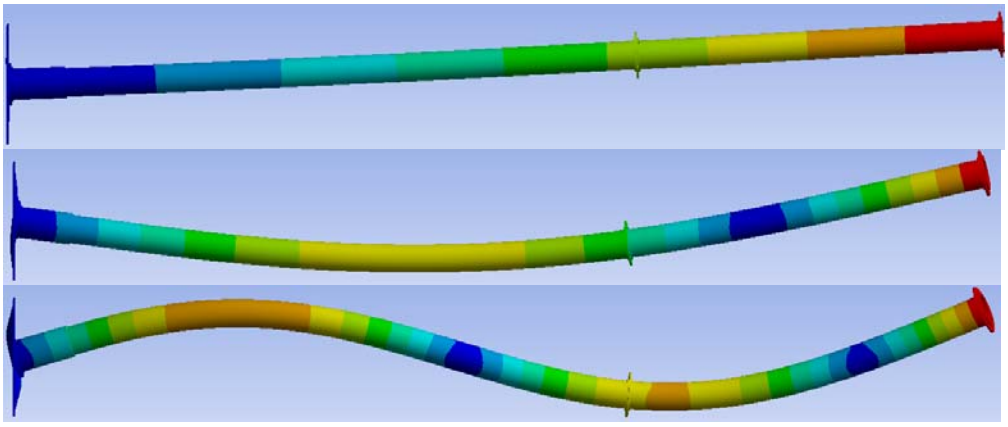

Figure 48: FE mode shapes of clamped pipe

5.5 Tube with blades

Below the FE and experimental results are compared.

5.5.1 FE mode 1 and 2

Table 33: Experimental Eigen frequencies and mode shapes, and FE model Eigen frequency of mode 1 and 2 of the pipe and blade assembly

FEM	Experiment	
Eigen fr.	Eigen fr.	Mode shape
2.29 Hz	2.25 Hz	Side-Side/Fore-aft
2.33 Hz		

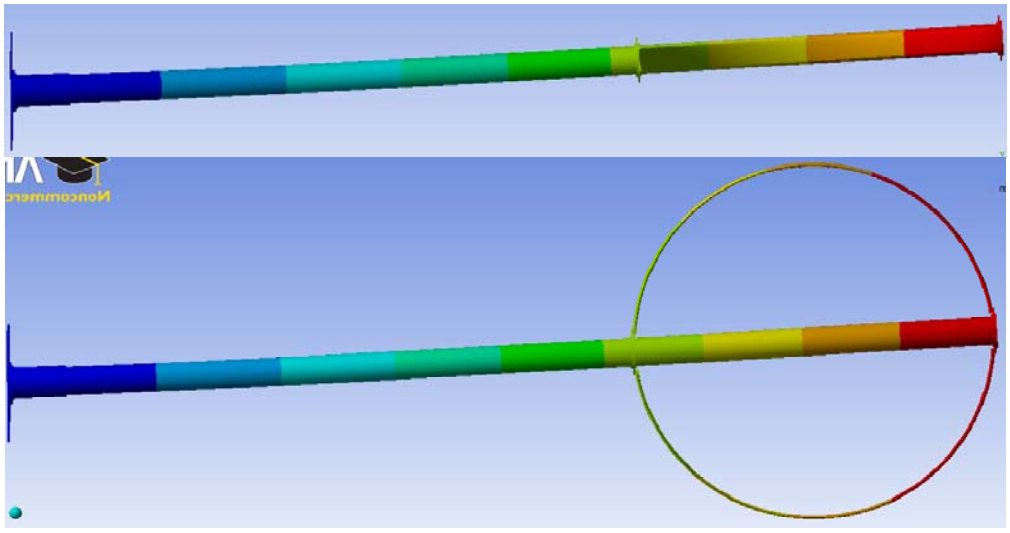

Figure 49: Mode shape 1 and 2 of the fixed support model of pipe and blade assembly

5.5.2 FE mode 3, 4 and 5

Table 34: Experimental Eigen frequencies and mode shapes, and FE model Eigen frequency of mode 3, 5 and 5 of the pipe and blade assembly

FEM	Experiment	
Eigen fr.	Eigen fr.	Mode shape
19.73 Hz	16.75 Hz	Second Tube bending
20.41 Hz	18.00 Hz	Torsion
21.45	-	-

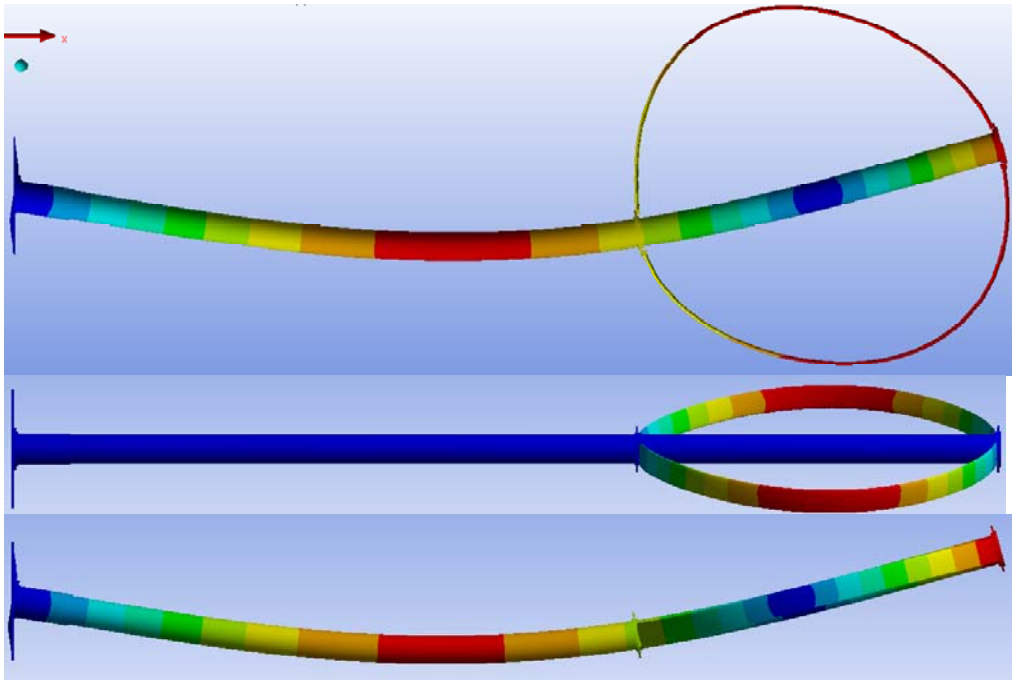

Figure 50: Mode shape 3, 4 and 5 of the fixed support model of pipe and blade assembly

5.5.3 Mode 6, 7 and 8

Table 35: Experimental Eigen frequencies and mode shapes, and FE model Eigen frequency of mode 6, 7 and 8 of the pipe and blade assembly

FFM	Experimen	
Eigen fr.	Eigen fr.	Mode shape
30.12 Hz	33.25 Hz	Uncertain, primary blade motion
32.58 Hz		
49.34 Hz	42.25 Hz	Uncertain, primary blade motion

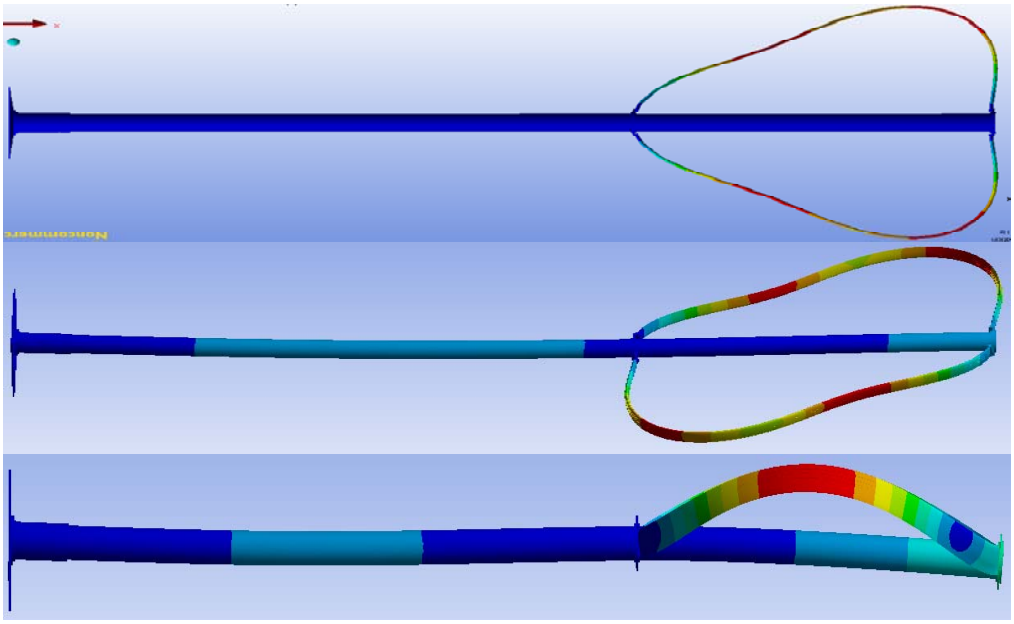

Figure 51: Mode shape 6, 7 and 8 of the fixed support model of pipe and blade assembly

5.5.4 Mode 9 and 10

Table 36: Experimental Eigen frequencies and mode shapes, and FE model Eigen frequency of mode 9 and 10 of the pipe and blade assembly

FEM	Experiment	
Eigen fr.	Eigen fr.	Mode shape
62.41 Hz	60.00 Hz	Uncertain, Primary tube
66.2 Hz		

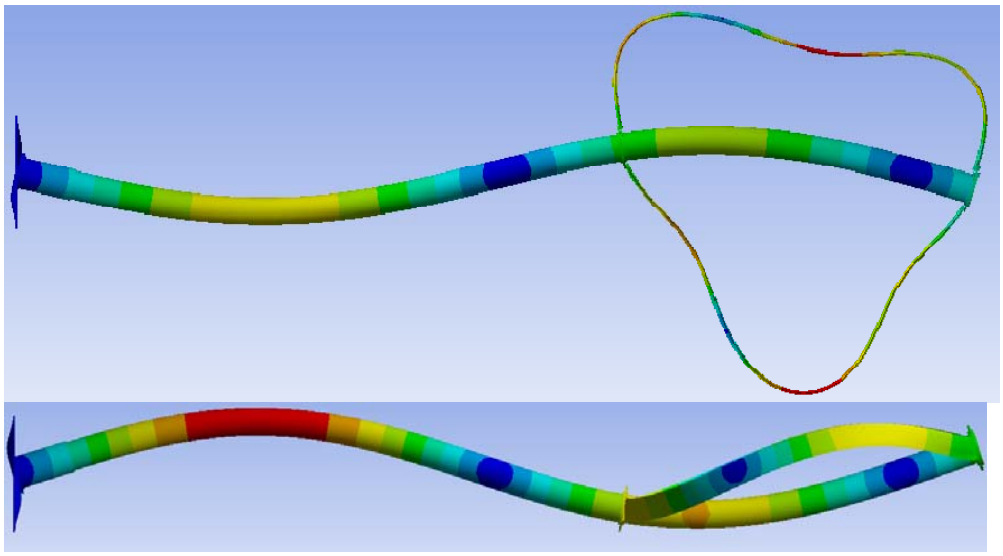

Figure 52: Mode shape 9 and 10 of the fixed support model of pipe and blade assembly

As seen from the results, there is generally a good agreement between the FE and the experimental results.

5.6 Tube and blades on rotating support

In table 37, the frequencies of the fixed support model are compared to the frequencies of the hinged support model.

Table 37: Eigen frequencies of the fixed support model compared to Eigen frequencies of the hinged support model.

Fixed support	Hinged suppor:	Mode shape
2.29 Hz	4.5181 Hz	Fore-aft
2.33 Hz	- Hz	Side-side
19.73 Hz	15.035 Hz	2nd tube bend ng s-s
20.41 Hz	- Hz	Torsion
21.45 Hz	30.429 Hz	2nd tube bend ng f-a
30.12 Hz	31.558 Hz	1st blade assym flap
32.58 Hz	32.953 Hz	1st blade sym flap
49.34 Hz	50.225 Hz	1st b ade edge sym
62.41 Hz	44.157 Hz	3rd tube bending s-s

From table 34 it is seen that the side-side mode disappears because of the hinged, zero-stiffness support. The frequencies of the fore-aft bending modes are increased because the hinged support is supported in the hinges and zero hinge displacement is prescribed. The torsional frequency disappears because the pipe-blade assembly is free to rotate.

5.6.1 Campell Diagram

The Campell diagram of the hinged pipe and blade assembly is estimated and shown in figure 53. As seen from the figure, there are 4 potentially critical rotational frequencies: The 1P, 2P and 3P crossing of the first Eigen frequency (side-side), and the 3P crossing of the second Eigen frequency (side 2nd pipe bending).

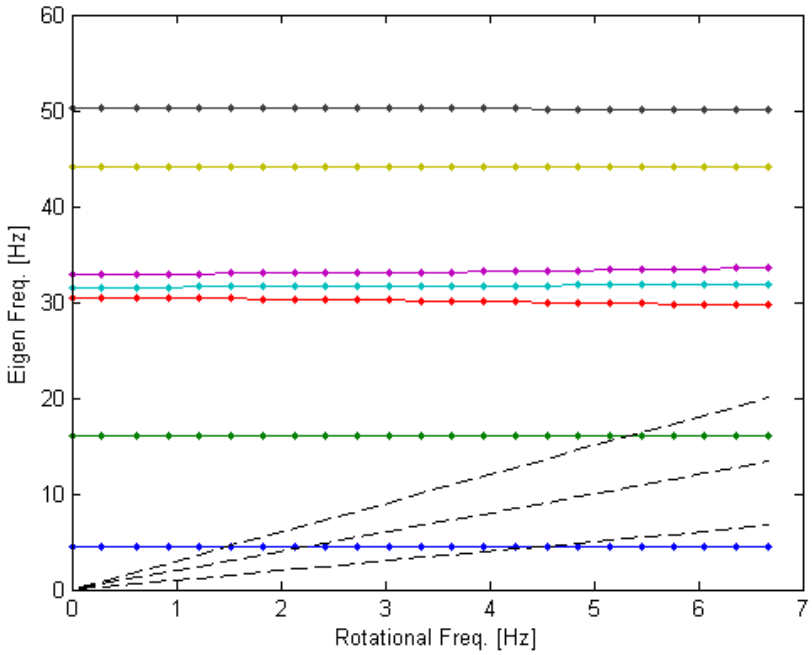

Figure 53: Campell diagram of the model with hinged support. The dashed lines indicate the 1P, 2P and 3P frequency.

5.6.2 Uncertainties

The results are associated with uncertainties due to some un-modelled features. The un-modelled features are summarized below and the expected effects of the un-modelled features are introduced. The likely effects of the un-modelled features on the Campell diagram are illustrated in figure 54-56.

- No fluid structure interaction between the submersed structure and the surrounding fluid.
    - The side-side mode of the pipe is in the model a rigid body motion with zero frequency. The fluid-structure interaction will increase the frequency of the side-side mode due to the buoyancy of the pipe, and the side-side frequency will be visible in the Campell diagram.
    - The pipe frequencies will be slightly decreased due to the damping of the fluid interaction
- On the real demonstrator, the hinged support is mounted at the end of a buoyant support beam. Thus, the stiffness of the hinged support around the axis that is perpendicular to the hinge axis will be less than infinity, which is assumed in the model
    - The less stiffness will lead to lower fore-aft frequencies
    - The support beam is hinged at its supported end, and allows the pipe-blade assembly to move along the vertical axis (heave). Thus the support beam will give rise to an additional, slow frequent mode.

Likely effects of uncertainties on Campell diagram

The effects of the uncertainties are indicated with arrows in the figures below

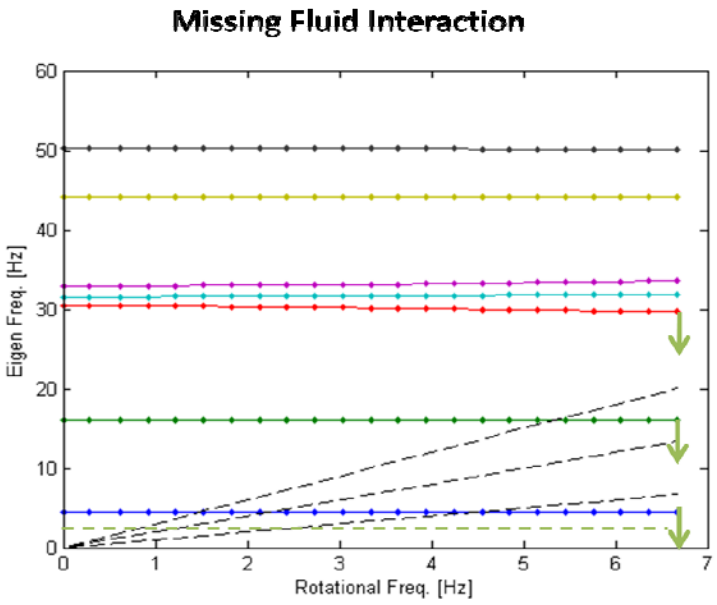

Figure 54: Likely effects of the un-modelled fluid-structure interaction on the Eigen frequencies.

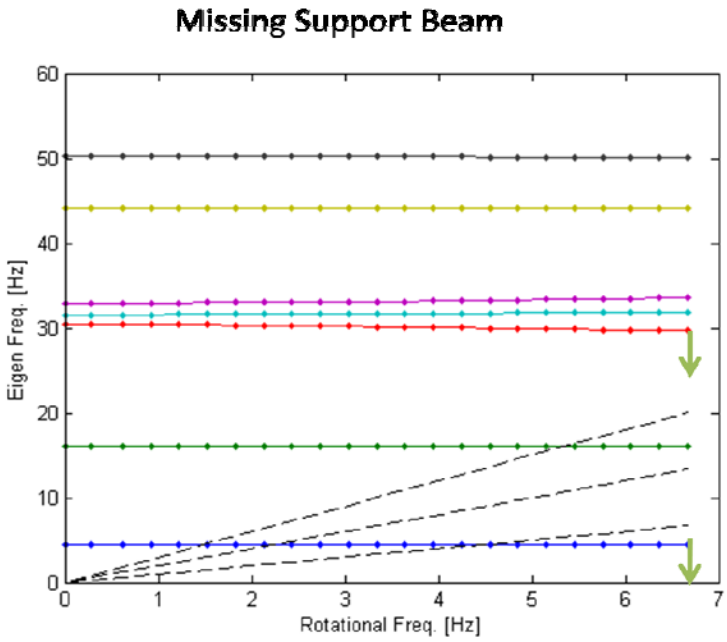

Figure 55: Likely effects of the un-modelled support beam on the Eigen frequencies.

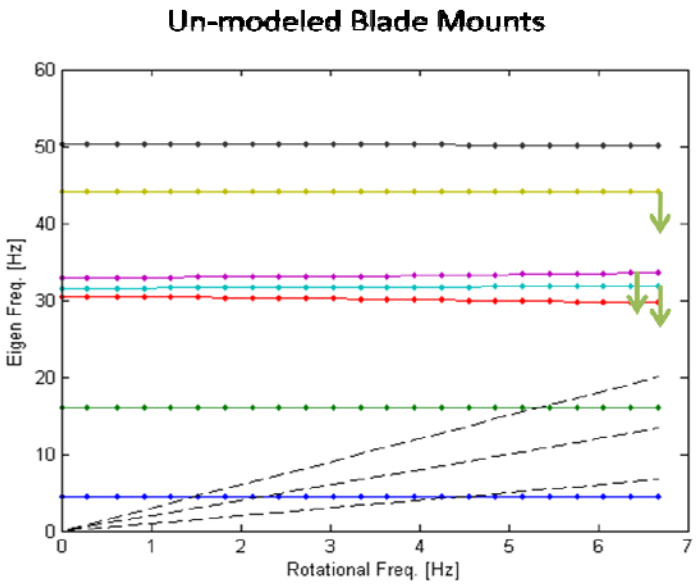

Figure 56: Likely effects of the un-modelled blade mount flexibility on the Eigen frequencies.

5.7 Conclusions on structural dynamics

In this study, the estimate of the Campell diagram and mode shapes of the Deep Wind demonstrator has been developed. Uncertainties relating to the model have been identified and the likely effects of the uncertainties have been described. It is recommended that the further studies are performed using the aero elastic simulation tool HAWC2 that enables estimation of the Eigen frequencies of the structure under the influence of both aero- and hydrodynamics.

6. Test site Roskilde Fjord

6.1 Location of the test site

The test site in Roskilde Fjord is close to Risø campus laboratories. In order to find the best suitable position the sea bed characteristics and water depth in the area around the pier at Risø was investigated with respect to depth and sea bottom characteristics. The best position was 50m west of the pier. The water depth at the position is 4m, plus a layer of soft mud of about 0.5m. Therefore a distance of 4.5m from the mean water level to the hard sea bed was considered. The position on a sea chart is shown in figure 57. The position was market with a yellow sea mark positioned 25m west of the demonstrator position. In figure 58 the position is shown, seen from west towards the Risø campus pier.

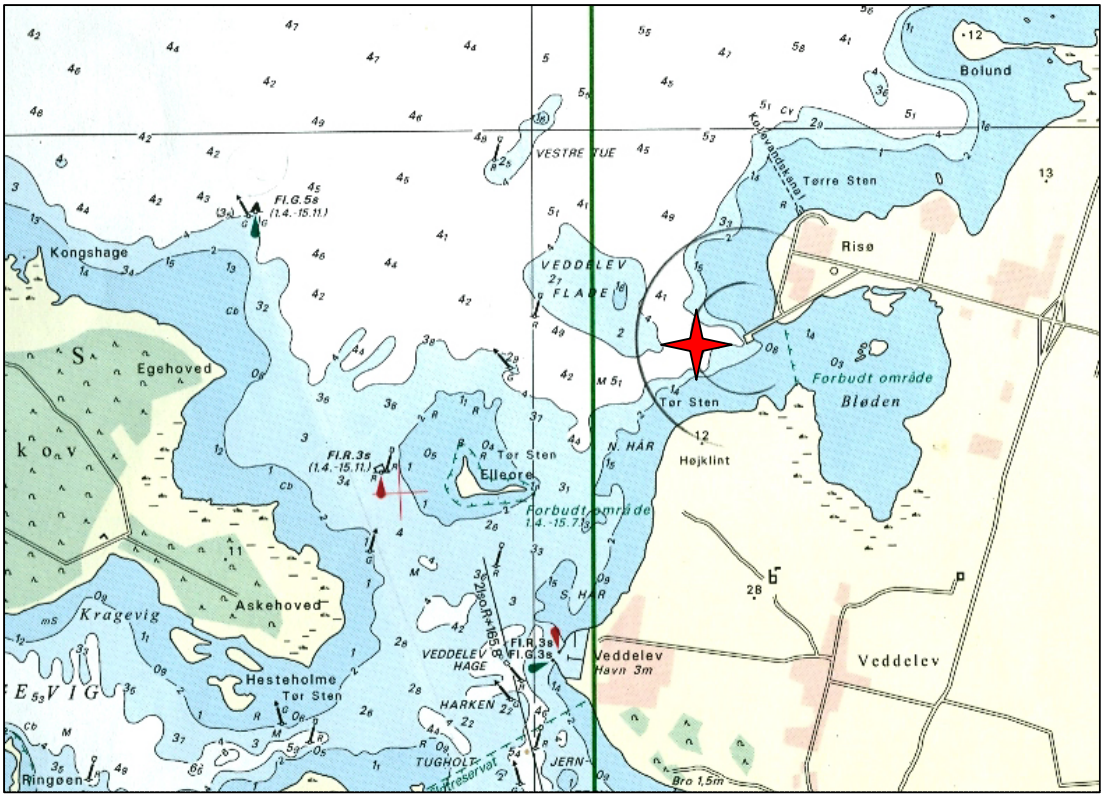

Figure 57: Location of test site for DeepWind demonstrator 50m west of Risø campus pier.

6.2 Wind resource at test site

A study by Trento on the wind resources at the test site was made. The rotor centre is about 2m above the water surface. This height has been used to make a first estimate of the mean wind velocity experienced by the rotor.From the Risoe meteorological database the mean wind velocity at 125m at the met mast is 7.82m/s (data from 1996 to 2000). Supposing the same mean wind velocity at 125m above the sea surface and a roughness parameter z0 between 0.001 (Risoe guidelines) and 0.01 a mean wind speed of about 5.0m/s is found. With an average wind speed of 5m/s at the rotor centre and a Weibull shape parameter of 2 the probability density function (pdf) and the cumulate (C) are depicted in figure 59.

Figure 58: Location of test site for DeepWind demonstrator 50m west of Risø campus pier, seen from west.

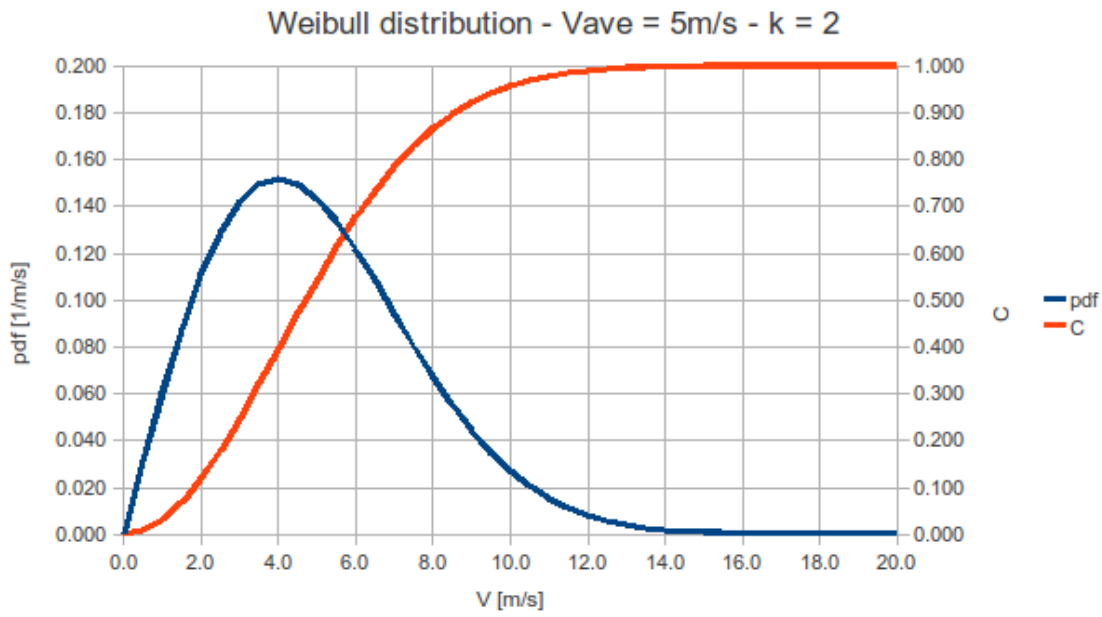

Fig. 59 Probability density function and cumulate of a Weibull distribution with a 5m/s average wind speed and a shape parameter *k* = 2.

Looking at figure 59 it can be seen that in order to maximize the number of hours in working conditions the cut in wind speed should be kept quite low (possibly lower than 4m/s to have the turbine working at least 60% of time). To improve the self-starting capability any mechanical friction should be kept as low as possible. A design wind speed, following the standard IEC61400-2, is taken as 1.4xVave = 7m/s. This was used in the design calculations [5].

6.3 Waves and currents at test site

DHI have forecasted the maximum wave height [13] at the site to be H_s=0.9m, assuming a water depth of 5m at the test position. The corresponding peak period (based on a wind generated wind spectra, i.e JONSWAP formulation) is T_p=3.2s. Figure 60 shows maximum wave heights in Roskilde Fjord.

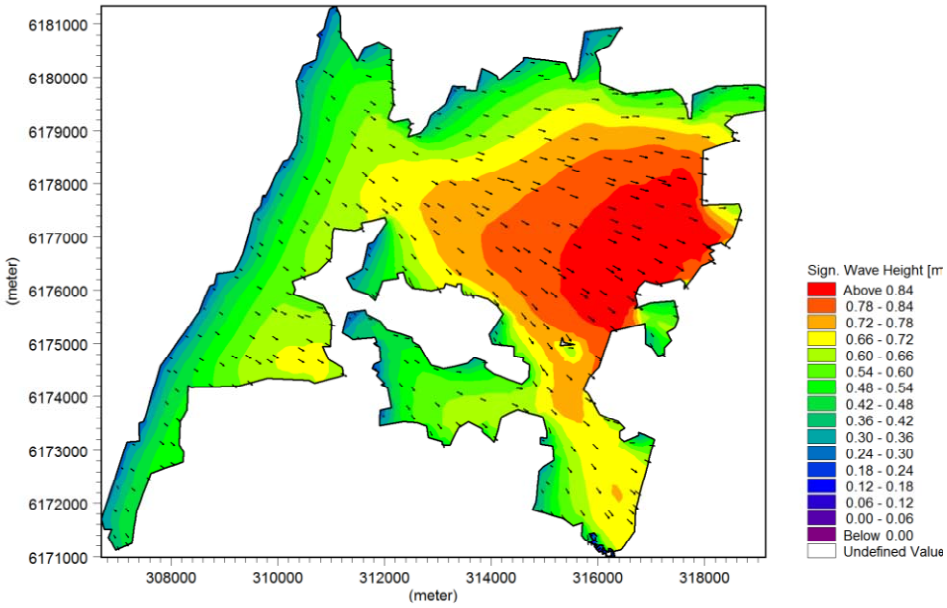

Figure 60 Expected wave height at Roskilde Fjord, from[13]

In the same report [13], the maximum value of the water currents at the site is estimated to be below 0.1m/s (height averaged water speed), see figure 61.

Other characteristic parameters are calculated using linear wave theory, see [9]. A list of the wave characteristic numbers expected at Risø fjord, is listed in table 17.

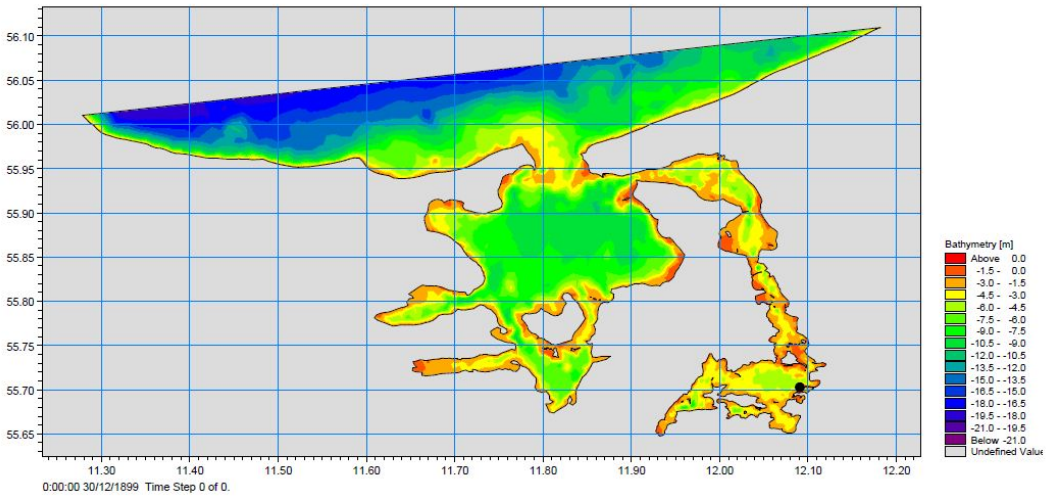

Figure 61 Expected currens at Roskilde Fjord, from [13]

6.4 Test plan at Roskilde fjord

The test plan for the tests in Roskilde fjord should take advantage of the special conditions at the location. From west to north the waves have a long fetch to gain height while from north east to southwest the fetch is short and waves are small. Continuous operation of the wind turbine was not possible, so only a limited number of datasets should be made while being manually controlled. The wind was then divided into three categories, low wind, average wind and high wind. For these three categories of wind and the two categories of waves a test matrix was made as the test plan to cover the important load cases, see table 38.

Table 38 Test matrix for wind and waves at Roskilde fjord experiments

Wind and wave matrix	Low wind below 8m/s	Average wind 8m/s to 11m/s	High wind 11m/s to 16m/s
Winds from E, SE and S (low waves)	Case 1	Case 3	Case 5
Winds from W and NW (high waves)	Case 2	Case 4	Case 6

6.5 Deployment and service operations

For deployment of the demonstrator a service vessel was made. The vessel was made of aluminium. Two tubes were connected in a catamaran configuration so that the vessel could go around the mast to position it in the middle, see figure 62. A lifting device could then lift the whole construction in one peace and transport it to the exact test site position 50m west of the pier.

Figure 62 The service vessel with the mast in the middle

Deployment of the demonstrator was made with a truck crane. First the foundation with mast, torque arm and generator box was lifted into the water next to the pier, see figure 63. Then the whole construction was lifted with the service vessel and transported to the site with another boat, see figure 64.

Figure 65 shows a situation with ice on the sea surface when the demonstrator was taken back again in November 2012. The rotor was sunken a little due to the temperature change of the air in the air barrels in the torque arm.

Figure 63 Deployment of the demonstrator by truck crane to the sea next to the pier

Figure 64 Transport of the demonstrator to the test site position with the service vessel and a boat

Figure 65 Ice conditions at the test site when the demonstrator was about to be transported back to the pier

7. Conclusions

A demonstrator wind turbine of 1kW and a rotor of 2x2m has been designed and manufactured for proof-of-concept tests of the DeepWind wind turbine concept in Roskilde fjord in waters of 5m depth and in a test basin at Marin with variable depth. The wind turbine was designed in two steps, and furthermore, the design was changed during manufacture. The first blades were not satisfactory and alternative blades were provided. This resulted in two sets of blades; one set of extruded aluminium blades with a chord of 0.10m and another set of GRP blades of 0,12m. The rotor is in total 5m long. The designed rotor tube thickness was not possible to deliver. An alternative 40% thicker wall thickness was provided on the tube, but this made the rotor heavier, and this required further changes. A 400mm diameter foam buoyancy part was added, and this has increased the friction in the water of the rotor. An asynchronous 4-pole generator is connected to the shaft via a belt with a gearing ratio of 1:3.4. Structural dynamics of the turbine was investigated theoretically and experimentally, and resulted in satisfactory structural dynamic behaviour.

8. References

1) Vita, L., Paulsen, U. S., Pedersen, T. F., Madsen, H. A., and Rasmussen, F., “A novel floating offshore wind turbine concept”. In Proceedings of the EWEC, European Wind Energy Conference, Marseille, France, 2009.
2) Vita, L., Paulsen, U.S., Pedersen, T.F., “A novel floating offshore wind turbine concept: new developments”. In Proceedings of the EWEC, European Wind Energy Conference, Warzaw, Poland, 2010
3) Jonkman J, “DeepCwind Scaling Laws”, NREL kick-off meeting presentation
4) Batista L, Zanne L “Aerodynamic design of the 2m diameter Darrieus wind turbine”, deliverable D1.2-D7.1 of the DeepWind project
5) Batista L, Zanne L, Brighenti A, “Second aerodynamic design of the 2m diameter Darrieus wind turbine”, deliverable D1.2 – D7.1 of the DeepWind project
6) Vita, L, “Notes, data and considerations on DeepWind demonstrator” April 2011, DTU internal note
7) M.C. Classens “The design and testing of airfoils for application in small vertical axis wind turbine”, TUDelft MSc Thesis, 2006
8) Carstensen S, DHI internal DeepWind report, 2011
9) Vita L, “Design and Aero-elastic Simulations of a 1kW Floating Vertical Axis Wind Turbine”, Risø-I-3204(EN), September 2011, technical report
10) Hørlyck P, “Evaluation of blades for demonstrator delivered from Nenuphar”, oktober 2012, internal DeepWind report
11) Klimas PC “Tailored airfoils for vertical axis wind turbines”, SAND84-1062 UC-60, February 1992
12) Kragh K, Finite Element Modal Analysis of the DeepWind Demonstration Model, August 2012, Internal DeepWind report
13) Carstensen J, DeepWind – DHI Input to WP7 Specifications, April 2011

Further documents than the ones referenced above were provided during the work:

14) Vita L, “Offshore floating vertical axis wind turbines with rotating platform”, PhD thesis, Risø DTU, Technical University of Denmark, August 2011, PhD-80(EN)
15) Vita L, Zalhe, F., Paulsen, U., Pedersen, T. F., Madsen, H., and Rasmussen, F., 2010. “A novel concept for floating offshore wind turbine: recent developments in the concept and investigations on fluid interaction with the rotating foundation”. In Proceedings of the ASME 29th International Conference on Ocean, Offshore and Arctic Engineering, Shanghai, Vol. 3, ASME.

9. Appendix Demonstrator drawings

DTU Vindenergi er et institut under Danmarks Tekniske Universitet med en unik integration af forskning, uddannelse, innovation og offentlige/private konsulentopgaver inden for vindenergi. Vores aktiviteter bidrager til nye muligheder og teknologier inden for udnyttelse af vindenergi, både globalt og nationalt. Forskningen har fokus på specifikke tekniske og videnskabelige områder, der er centrale for udvikling, innovation og brug af vindenergi, og som danner grundlaget for højt kvalificerede uddannelser på universitetet.

Vi har mere end 230 ansatte og heraf er ca. 60 ph.d. studerende. Forskningen tager udgangspunkt i 9 forskningsprogrammer, der er organiseret i tre hovedgrupper: vindenergisystemer, vindmølleteknologi og grundlag for vindenergi.

Technical University of Denmark
DTU Vindenergi
Frederiksborgvej 399
Bygning 125
4000 Roskilde
Telefon 45 25 25 25
info@vindenergi.dtu.dk
www.vindenergi.dtu.dk